AAEC/E165

AAEC/E165

30

AUSTRALIAN ATOMIC ENERGY COMMISSION

RESEARCH ESTABLISHMENT
LUCAS HEIGHTS

THE EXPERIMENTAL DESIGN OF TESTS TO MEASURE THE THERMAL STRESS RESISTANCE OF SPHERICAL CERAMIC FUEL ELEMENTS FOR NUCLEAR REACTORS

by

J. C. M. JONES

November 1966

AUSTRALIAN ATOMIC ENERGY COMMISSION
RESEARCH ESTABLISHMENT
LUCAS HEIGHTS

THE EXPERIMENTAL DESIGN OF TESTS TO MEASURE THE THERMAL STRESS RESISTANCE OF SPHERICAL CERAMIC FUEL ELEMENTS FOR NUCLEAR REACTORS

by

J.C.M. JONES

ABSTRACT

The statistical and thermodynamic problems introduced in quench testing the thermal stress resistance of spherical ceramic fuel elements for nuclear reactors are analysed.

The statistical problem is one of deciding how many specimens to quench in order to achieve a required confidence interval in the working stress deduced from the test. Two methods are considered: Quantal Response and the Up-and-Down Methods. Estimates of confidence interval associated with a range of sample sizes are obtained by a computer simulation technique. It is shown that sample sizes of several hundred specimens would be required in order to obtain confidence intervals compatible with demands of reactor design.

The thermodynamic problem is one of predicting the specimen temperature distribution from which the stress may be calculated. A solution for the case of the single specimen is already available. Multiple specimens, which offer the advantage of shortening the time scale of the experiment, introduce the problem of a time dependent quenchant temperature; a solution, in terms of heat regenerator theory, is presented.

CONTENTS

1. INTRODUCTION

The attainment of high gas coolant temperatures in nuclear reactors requiring a moderator may necessitate the use of ceramics as moderator material and fuel containment. An example of such an application is the Pebble Bed High Temperature Gas–Cooled Reactor which has been under study by the Australian Atomic Energy Commission (Roberts 1964). The fuel elements are beryllium oxide spheres of 1 to 1½ inches diameter containing the fissile material as a particulate dispersion. It has been shown by Wright (1964) that the thermal stress capability of such fuel elements is important in reactor economics; consequently a working thermal stress that exploits the material to the full must be specified.

Apart from the inherent uncertainties in predicting thermal loading in a nuclear heated gas–cooled pebble bed; for example, the effect of random packing on the coolant flow distribution; the main difficulty in predicting the thermal stress resistance of ceramic fuel elements is that the strength is dependent on such characteristics as loading, size, shape, and manufacturing route. Thus, strength data must be obtained on production specimens thermally loaded in a manner closely simulating service. For spherical shapes this implies either in–pile experiments or quenching as the next closest approximation offering significant economies in the cost of the apparatus. The latter alternative is considered in this paper, although some of the aspects discussed are applicable to both.

Quench testing introduces experimental problems in two areas:

(i) Thermodynamics, namely the prediction of heat removal rate during the quench process, the effect of temperature dependent properties, and the role of non–uniform heat removal in the thermal stress history.

(ii) Statistics, namely the number of tests required to achieve a given confidence interval determined by the sensitivity of in–service failure rate to inaccuracies in specified design stress.

In the following detailed treatment the statistical aspect is dealt with first because the number of specimens required could have a significant influence on the type of experiment chosen.

2. SENSITIVITY OF FAILURE RATE TO APPLIED STRESS

The concept of designing a ceramic component to a given service failure rate is a consequence of the observed significant scatter in material strength properties. Thus, were the design stress to be set at the median strength value, half the components would fail in service. In the case of elastic non–brittle materials, for example steels, this is not a problem, because the scatter band is so narrow that a slight lowering of the design stress reduces the failure rate to almost zero. On the other hand, high quality reactor–grade ceramics may show coefficients of variation as high as 15 per cent. and the design stress would have to be reduced to 55 per cent. of the median in order to reduce the failure rate to, say, between 1 and 2 per thousand. This represents a significant degradation of material strength capability.

To illustrate this situation, Figure 1 shows the effect of applied stress level on the failure rate for two materials having different strength distributions. The first, referred to as the linear normal model, has a normal distribution of the strength about the mean given by the integral:

$$\text{Failure rate at applied stress } S_1 = P_1 = \frac{1}{\sigma_0\sqrt{2\pi}}\int_{-\infty}^{S_1} \exp\left[-\frac{(S_1-\mu_0)^2}{2\sigma_0^2}\right]dS \,, \qquad (1)$$

where μ_0 = mean strength

σ_0 = standard deviation of the strength about the mean.

The second, referred to as the log normal model, has the natural logarithm of the strength normally distributed about the natural logarithm of the mean, as in Equation 1, except that S_1, μ_0, and σ_0 are expressed as logarithms. This model may be more applicable to the failure statistics of beryllium oxide. For instance, experiments by Rotsey and Veevers (unpublished) on sintered material has indicated a strength–porosity relationship of the form:

$$\sigma = \sigma_0 \exp(-Kp)$$

where σ_0 = strength of non-porous material

K = a positive constant

p = porosity

If the porosity is normally distributed, it may be shown that the natural logarithm of the strength will also be normally distributed. It should be pointed out that verification of the applicability of a particular model when the desired failure rate is low (say 10^{-5} to 10^{-3}) would require many thousands of tests. Generally, indirect evidence must be sought in support of a particular model.

The curves in Figure 1 show that in the range 1/1000 to 1/100 the failure rate is very sensitive indeed to applied stress. For example, an increase of 5 units (say 10 per cent.) in the applied stress trebles an initial failure rate of 1/1000 in the case of the linear normal model and quadruples it in the case of the log normal model. If surface failure of reactor fuel elements releases fission products to the coolant, this increase of failure rate would be considered significant. The implication is that the design stress value should be known to better than 10 per cent. Figure 2 shows a similar set of curves, except that a statistical variation of applied stress has been included. This would correspond to the situation in a pebble bed being continuously charged at the top and discharged at the bottom, the pebbles being subjected to a random component of applied stress on their way down. The applied stress distribution has been assumed normal, with standard deviations of 5 units, 10 units, and 5 per cent. of applied stress. Again, the failure rate is very sensitive to applied stress, especially for the latter condition, which would correspond to, say, the case of thermal stress variations due to non-uniform heat transfer over the ball.

3. THE STATISTICS OF QUENCH TESTING

The underlying difficulty of quench testing is that the stress level at the moment of failure is not known. The situation is exactly analogous to that in toxicology when, for example, the potency of pesticides is being tested. In both cases it is scientifically unsound to test a given specimen more than once, because there is no certainty that the result of a subsequent test would be independent of a previous one.

Thus, recourse must be had to a statistically designed test in which the result of a number of trials is observed as fail or not-fail and from which an estimated value of the mean strength and its standard deviation may be obtained. There are two approaches.

One approach, the "Quantal Response Method", is to divide the test specimens into several groups which are each quenched at one of a set of stresses around a guessed value of the mean. A normal failure model is then assumed and, in the more elementary investigations, the mean and standard deviation are deduced by plotting on probability paper the proportion of failures in each group versus applied stress. The disadvantage that the groups of specimens showing complete failure or non-failure are lost to the analysis can be overcome by a numerical rather than graphical approach which uses all the data, known as Probit Analysis (Finney 1962).

As alternative approach is a sequential one known as the "Up-and-Down Method", described by Dixon and Mood (1948). The first specimen is quenched at a stress equal to a guessed value of the mean and, depending on whether failure occurred or not, the next specimen is quenched at a lower or higher stress, respectively. The process is continued until the whole of the sample has been tested. The "test interval", that is, the amount by which the stress is raised or lowered between successive quenches is chosen as approximately equal to the standard deviation of the material strength. As would be expected, the test stress levels tend to cluster around the mean; the disposition of these test points may be analysed to give the mean and standard deviation. As in Probit Analysis, a normal model is assumed.

3.1 Outline of Theory

3.1.1 Probit Analysis

Equation 1 may be re-written:

$$P_1 = \frac{1}{\sqrt{2\pi}} \int_{-\infty}^{t_1} \exp\left(-\frac{t_1^2}{2}\right) dt \quad , \tag{2}$$

where $$t_1 = \frac{S_1 - \mu_o}{\sigma_o} = bS_1 + a \quad , \quad \text{say.} \tag{3}$$

Thus for observed proportions of failures $p_1, p_2, \ldots p_m$ corresponding to m groups of quenches at applied stresses $S_1, S_2 \ldots S_m$, $t_1 \ldots t_m$ may be obtained from tables (Fisher and Yates 1957). A plot of $t_1 \ldots t_m$ versus $S_1 \ldots S_m$ will be a straight line of slope $b = 1/\sigma_1$ and intercept $a = -\mu_1/\sigma_1$, where μ_1 and σ_1 are estimates of the population mean μ_o and standard deviation σ_o.

Paradine and Rivett (1964) show, by applying χ^2 tests, that the "best" estimate of μ_o and σ_o is not that obtained by the straightforward least squares fit; the "best" estimate is given by a weighted fit in which account is taken of the "statistical worth" of the experimental points. Briefly, the argument, developed in detail by Finney (1962), runs as follows:

For any given value of stress, let there be r failures from n quenches, that is, the proportion of failures = p_r, say, = r/n. Proportion is synonymous with probability and since the probability of r failures in n quenches is binomially distributed, the following relationship holds:

$$p_r = {}^nC_r \, P^r \, Q^{n-r} \quad , \tag{4}$$

where P is the expected probability of failure predicted from Equation 2 and Q is the probability of non-failure, equal to 1-P. Thus the likelihood of obtaining any observed combination of m results is given by the compound probability:

$$1 = p_{r_1} p_{r_2} \ldots p_{r_m} \quad . \tag{5}$$

The problem is now to determine the values of a and b which maximise this likelihood; these values would then be the statistically best estimates of a_o and b_o. A successive approximation approach is necessary and Finney proves that if a_1 and b_1 are first approximations to a and b and:

$$\left.\begin{aligned} t_i &= b_1 S_i + a_1 \\ Z_i &= \frac{1}{\sqrt{2\pi}} \exp\left(-\frac{t_i^2}{2}\right) \\ P_i &= \frac{1}{\sqrt{2\pi}} \int_{-\infty}^{t_i} \exp\left(-\frac{t_i^2}{2}\right) dt \\ Q_i &= 1 - P_i \\ p_i &= \frac{r_i}{n_i} \quad , \quad \text{as defined previously,} \end{aligned}\right\} \tag{6}$$

then:

$$\left.\begin{aligned} a_2 \sum_{i=1}^{m} \frac{n_i Z_i^2}{P_i Q_i} + b_2 \sum_{i=1}^{m} \frac{n_i Z_i^2 S_i}{P_i Q_i} &= \sum_{i=1}^{m} \frac{n_i Z_i^2}{P_i Q_i} \left(\frac{p_i - P_i}{Z_i} + t_i\right) \\ \text{and} \\ a_2 \sum_{i=1}^{m} \frac{n_i Z_i^2 S_i}{P_i Q_i} + b_2 \sum_{i=1}^{m} \frac{n_i Z_i^2 S_i^2}{P_i Q_i} &= \sum_{i=1}^{m} \frac{n_i Z_i^2 S_i}{P_i Q_i} \left(\frac{p_i - P_i}{Z_i} + t_i\right) \end{aligned}\right\} , \tag{7}$$

where a_2 and b_2 are a closer second approximation to a and b. The process may be repeated until asymptotic values of a_2 and b_2 are found.

Equations 7 correspond to a weighted least squares fit on the line $a_2 + b_2 s = \frac{p - P}{Z} + t$. The unweighted least squares fit is obtained by eliminating the weights $\frac{nZ^2}{PQ}$ and noting that $\sum_{i=1}^{m} \frac{p_i - P_i}{Z_i} \to 0$ for large m.

A method is available (Whitaker and Robinson 1962) for calculating the variances of the deduced mean and standard deviation obtained from a given set of data as described above. Thus confidence intervals could be retrospectively estimated. However the problem of predicting the variances for a given experimental scheme does not appear to be analytically soluble. Simulation provides an alternative approach; results obtained by this technique are described in Section 3.2.

3.1.2 The Up-and-Down Method

As before, the strength or some prescribed function of the strength of the material is assumed normally distributed. The stress level S_o of the first quench corresponds to the guessed mean strength of the material and the other stress levels are given by:

$$S_i = S_o \pm id \quad , \qquad i = 0, 1 \tag{8}$$

where d is the interval between levels (the "test interval"). The probability of any given set of responses, given a first stress level S_o is given by:

$$P\,(f,g|S_o) = K \prod_{\text{all } i} \left(P_i^{f_i} Q_i^{g_i}\right) \quad , \tag{9}$$

where f_i and g_i are the number of failures and non-failures at stress level S_i and P_i respectively, Q_i are as defined previously, and K is a constant not a function of μ_o and σ_o.

Assuming large samples and an initial stress level close to the mean:

$$P\,(f,g|S_o) = K \prod_{\text{all } i} (P_i\, Q_i)^{g_i} \tag{10}$$

Applying the principle of maximum likelihood, $P\,(f,g|T_o)$ is differentiated with respect to μ_o and σ_o and the results are equated to zero:

$$\left.\begin{aligned} \sum_{\text{all } i} g_i \left(\frac{Z_i}{Q_{i-1}} - \frac{Z_i}{P_i}\right) &= 0 \\ \sum_{\text{all } i} g_i \left(\frac{t_{i-1} Z_{i-1}}{Q_{i-1}} - \frac{t_{i-1} Z_i}{P_i}\right) &= 0 \quad , \end{aligned}\right\} \tag{11}$$

where Z and t are defined as before, the suffix in this instance referring to the number of trial intervals up or down from the first trial

It would be theoretically possible to solve for μ and σ by successive approximation. However Dixon and Mood (1948) show that, provided $d < 2\sigma$, estimates of μ_o and σ_o, say μ and σ, can be obtained from the following:

$$\left.\begin{aligned} \mu &= S^* + d\left(\frac{A}{N} \pm \frac{1}{2}\right) \\ \text{and} \qquad \sigma &= 1.620\, d \left(\frac{NB - A^2}{N^2} + 0.029\right) , \end{aligned}\right\} \tag{12}$$

where S^* is the lowest applied stress at which the lesser of the events, failure or non-failure, occurs, N is the lesser of the total number of failures or non-failures, A is the lesser of $\sum_{\text{all } i} i\, g_i$ and $\sum_{\text{all } i} i\, f_i$, and B is the lesser of $\sum_{\text{all } i} i^2 g_i$ and $\sum_{\text{all } i} i^2 f_i$. In the first expression the plus sign is used if $g_i > f_i$

and the minus sign if $g_i < f_i$. If $g_i = f_i$, either can be used, consistent with the values of A and B used. The analysis also gives estimates of the standard deviations of the mean and standard deviations:

$$\sigma_\mu = G\,\sigma_o/\sqrt{N}$$
$$\text{and} \qquad \sigma_\sigma = H\,\sigma_o/\sqrt{N} \quad , \quad \text{respectively,} \tag{13}$$

where G and H are functions of σ_o/d only, given a normal distribution model. From curves of these functions given by Dixon and Mood the maximum accuracy is obtained for a test interval $d \approx \sigma_o$.

It should be noted that these results apply to large samples and the authors point out that, in practice, this would imply a sample size of at least 40. Since the present investigation was concerned with reducing sample size within the constraint of the accuracy requirement and since bias was also of interest, estimates of the accuracy of the Up-and-Down Method have also been obtained by simulation.

3.2 Comparison of Quantal Response and Up-and-Down Methods

Simulation of the production of experimental data by manipulating random numbers provides a ready method of testing the statistical methods described above. For Quantal Response data as many random numbers between 0 and 1 are drawn as there are quenches in a group at a given stress level. The numbers less than or equal to the expected proportion failing are the "observed" number failing. This observed proportion will be binomially distributed with respect to the expected proportion. Up-and-Down data are generated by drawing a single random number between 0 and 1 for each trial. If it is less than the expected probability of failure at the particular stress level, the next quench is at the next lower level, or vice versa.

Estimates of the bias and accuracy of the analysed data are obtained by repeating the simulation a sufficiently large number of times and analysing these results. Standard deviations of deduced mean, standard deviations and working stress can be obtained in the usual way and, provided that large sample theory applies, an accuracy can be quoted, as, say, a 95 per cent. confidence interval, corresponding to a band enclosing the mean value, plus or minus twice its standard deviation. In the present paper it is so quoted as a percentage of the working stress. The implication is that any given experiment will give a result within this band 19 times out of 20. The applicability of large sample theory in such an analysis has been checked by plotting the frequency distribution of the results; this was found to be acceptably symmetrical in the cases of interest.

The two models of strength distribution, linear normal and log normal, were considered. The population mean strength was set at 100 units. The standard deviation for the linear normal model was varied over the range 5 to 20 units and for the log normal model over the range 0.05 to 0.2. Bias and accuracy were estimated for two predicted failure rates; a "low" failure rate of 1.35/1000 corresponding to a working stress of three standard deviations down from the mean and a "high" failure rate of 22.75/1000 corresponding to two standard deviations down from the mean. In the case of the log normal model, it is not strictly correct to quote a symmetrical accuracy about the mean, but the error by doing so is unimportant. In order to simplify the analysis of the results, only the linear normal model was used for comparison of various sampling schemes within a given method; in general, the results would also be applicable to the log normal model.

The bulk of the simulation of the Quantal Response Method was done on samples having nine stress levels, one at the mean and four each side at (standard deviation)/4 intervals. This choice was intuitive, but there is not much scope for other schemes; if the span is increased, the number of specimens required at the extreme stress levels must be increased in order to maintain selectivity. On the other hand, increasing the number of levels for a given sample size also reduces the selectivity. Reducing the number of levels reduces the number of points available for the Probit Analysis least squares fit. Simulation of the schemes other than the nine level scheme confirmed these predictions; these results are discussed. Apart from sample size, test interval is the only parameter in the Up-and-Down Method that can be varied. This was set at one standard deviation, near the optimum predicted by Dixon and Mood (1948). A few checks on other intervals were made, and are discussed.

The first important result of the simulation was that both the Quantal Response and Up-and-Down Methods show bias in the deduced value of working stress. The bias was almost entirely concentrated in the estimate of population standard deviation. Figure 3 summarises the working stress bias results; the Up-and-Down Method appears to show less bias and it is of opposite sign to that of the Quantal Response Method. For sample sizes required for acceptable accuracy, the bias would be between ±1 and ±2 per cent. In the present context, this would be considered just significant, and could be corrected simply by adding (or subtracting) the value appropriate to the observed population parameters and sample size as given by curves of the type shown in Figure 3.

The results of the calculations of confidence interval, or accuracy, of both methods are summarised on Figures 4, 5, 6 and 7 for the linear normal and log normal models, high and low failure rates. The salient features of these results are:

(i) Unless the standard deviation of the material strength is $\leqslant 10$ units for the linear normal model and 0.1 for the log normal model, sample sizes in the hundreds are required in order to obtain a 10 per cent. accuracy.

(ii) With high standard deviations, disproportionately large increases of sample size are required to improve the accuracy.

(iii) The accuracy given by the present simulation of the Up-and-Down Method is a factor of at least 2 worse than estimated by Dixon and Mood (1948). This discrepancy has not been explained.

A clearer comparison of trends is made in Figures 8 and 9, which are cross plots of the data shown previously. It is evident from these curves that the Up-and-Down Method requires significantly smaller samples than the Quantal Response Method, the reduction being in the range 30 to 50 per cent., which agrees with Dixon and Mood's predictions. Also, for a given working stress, the log model requires smaller sample sizes.

The implications of these results with respect to the design of quench experiments are as follows: Firstly, it is important to decide which model the failure strength distribution conforms to, as this has a significant effect on the sample size required. Secondly, if sample size is to dominate the experimental design, the Up-and-Down Method should be chosen. The associated disadvantage is the time required, because the stress level of the next test is dependent on the current one; thus tests have to wait on the results of sample inspection. Thirdly, if time is the dominant factor, the Quantal Response Method is the superior one, because a predetermined programme of tests can be followed independently of the results obtained. Furthermore, it is possible to design the test apparatus to quench many specimens at once, although this requires a more elaborate thermodynamic analysis, as is shown in the next section.

Both the Up-and-Down and Quantal Response Methods require an initial guess of the mean and the standard deviation. The consequences of a poor guess of the mean are not great in the Up-and-Down Method since the main outcome is a "waste" of a few specimens at the beginning in going from the initial stress level to one near the mean. With the Quantal Response Method, however, a poor guess results in a non-symmetrical distribution of stress levels about the mean. For example, a scheme corresponding to an error of (standard deviation)/2 in the guessed value of the mean for a sample size of 180 and a population standard deviation of 10, showed little deterioration in accuracy:

TABLE 1

EFFECT OF ASYMMETRY ON QUANTAL RESPONSE ACCURACY

$\sigma = 10$

Sample Size = 180

Central Point, Stress Units		95	100
Accuracy for low failure rate	% working stress	10.4	9.2
Accuracy for high failure rate		7.7	6.7

Increase of asymmetry beyond $\sigma/2$, however, apparently causes significant deterioration because the iterative procedure of the Probit Analysis required excessive computer time so that insufficient results were obtained. Thus permissible asymmetry is not very large, say 5 per cent. in the particular case discussed here. Given a situation in which the Quantal Response Method is preferred but the confidence interval of a guessed value of the mean exceeds $\pm\sigma/2$, the best approach would be to make a preliminary test using the Up-and-Down Method on a small sample in order to obtain a closer estimate. The Up-and-Down Method is particularly suited to this approach. For example, the following table gives the 95 per cent. confidence interval of the deduced mean of a population having a mean of 100 and a standard deviation of 10.

TABLE 2

ACCURACY OF MEAN FROM UP-AND-DOWN METHOD

$\sigma = 10$

Sample Size	Accuracy, % of Mean
20	6.3
30	5.2
40	4.8

Thus, a sample size of 40 would be adequate to obtain a preliminary estimate of the mean to within $\pm\sigma/2$. In order not to "waste" this data, the test interval could be set at, say $\sigma/2$, so that most, if not all, of the fail or not-fail results could then be combined with the main body of the Quantal Response information.

A poor guess of the standard deviation, and thus test interval, has little effect on the accuracy obtained from the Up-and-Down Method, as is demonstrated in the following table.

TABLE 3

EFFECT OF TEST INTERVAL ON ACCURACY OF THE UP-AND-DOWN METHOD

$\sigma = 10$ Sample Size = 50

Trial Interval	5	10	20	30
Accuracy, Low failure rate %	15.7	14.1	10.9	10.1
Accuracy, High failure rate %	11.6	10.5	8.5	8.5

In fact, the implication is that an improvement could have been obtained with a 2σ or 3σ test interval; this finding is contrary to Dixon and Mood's recommendations, but requires further investigations before a generalisation concerning the optimum test interval can be made. Without pursuing the matter further in this paper, we can, however, conclude that a "high" guess of σ is to be preferred to a low one, and that the available range of test interval would seem to be $\sigma/2$ to 2σ without significant loss of accuracy. The Quantal Response Method shows a similar trend of accuracy with test interval, as may be seen from the following table.

TABLE 4

EFFECT OF TEST INTERVAL ON QUANTAL RESPONSE ACCURACY

$\sigma = 10$ Sample Size = 180

Trial Interval	1.5	2.5	3.5
Accuracy, Low failure rate %	19.6	9.2	7.7
Accuracy, High failure rate %	14.1	6.7	5.7

It would appear that the choice of a test interval of 0.25σ was not so good, as say, 0.35σ for the particular sample size chosen for this comparison, but the scope for improvement is not great. The indications are, however, that a "high" guess of σ is to be preferred.

As the interest centres on the working stress corresponding to low failure rates, it may appear reasonable to bias the Quantal Response sample allocation to the low side of the mean. Such a scheme, having the following sample allocation, was tried: Mean = 100, σ = 10, Sample size 210.

Stress Level	82.5	85	87.5	90	92.5	95	97.5	100	102.5	105	107.5
Number of Specimens	70	50	30	20	14	10	7	6	5	4	4

The expected number of failures at each level was approximately the same. The accuracy of deduced working stress was calculated as 13.3 per cent. and 9.1 per cent. for the low and high failure rates, respectively, compared to 8.0 per cent. and 6.0 per cent. respectively for a symmetrical nine stress level scheme of the same sample size. Various other asymmetrical schemes were tried and it was found that no improvement over the symmetrical scheme could be obtained.

Finally, a five level symmetrical scheme was compared with a nine level scheme, and little difference between accuracies was found. For the sample sizes covered (up to 200) and the test interval ($\sigma/4$) selected, numbers of levels outside the range 5–9 tended to give a lower accuracy. This confirms the intuitive selection of a nine level scheme for the simulation.

4. THE THERMODYNAMICS OF QUENCH TESTING

A quenching experiment must take account of the need for large sample sizes. Thus, if some improvement in the time scale appropriate to quenching one specimen at a time in the same apparatus is required, the apparatus must either be multiplied several times so that quenches are carried out "in parallel" or a more elaborate apparatus must be devised which quenches many specimens at once, say "in series". The choice is mainly economic. The thermodynamics of single specimen quenching is well established, at least for spherical shapes of interest in the present work. The analysis of multiple specimens in series is more complex, because account must be taken of the functioning of the specimen as a heat regenerator, whose characteristics must be known in order to predict the thermal stress. On the other hand its behaviour may be exploited so that a single quench could impose the required range of stresses on a single sample of several hundred specimens. This represents a time saving of at least two orders over the single specimen quench.

The starting point in the analysis is the ideal situation corresponding to uniform heat removal and constant physical and thermodynamic properties of the quenchant and specimen. The departure from, and possible ways of accounting for departures from this ideal are then discussed in a general way; a detailed treatment is outside the scope of the present paper.

4.1 Single Specimens

Carslaw and Jaeger have presented a solution for the temperature distribution generated in a sphere quenched from uniform initial temperature, in a medium of constant temperature, the sphere surface heat transfer coefficient being uniform and constant. The physical properties of the sphere are also assumed constant. The solution is of the form:

$$\frac{T_{r,t}}{T_o} = 2.BN.\frac{R}{r}\sum_{i=1}^{\infty}\exp\left(-\frac{a\,\theta_i^2\,t}{R^2}\right)\left\{\frac{\theta_i^2 + (BN-1)^2\sin\theta_i\sin\left(\theta_i\frac{r}{R}\right)}{\theta_i^2\left[\theta_i^2 + BN(BN-1)\right]}\right\}, \qquad (14)$$

where:

$T_{r,t}$ = sphere temperature at radial position T , time t ,

T_o = initial sphere temperature, quenchant temperature being zero,

BN = sphere Biot Number, defined as $\frac{hR}{k}$,

where R = sphere radius,

h = surface heat transfer coefficient,

k = thermal conductivity of sphere,

a = thermal diffusivity of sphere = $\frac{k}{\rho_s C_{p_s}}$,

where ρ_s = density of sphere,

C_{p_s} = specific heat of sphere,

θ_i = is the i^{th} root of:

$$\theta_i \cot \theta_i + BN - 1 = 0 \tag{15}$$

At time t and radial position r the tangential and radial stresses, respectively ${}_t\sigma_{(r,t)}$ and ${}_r\sigma_{(r,t)}$ per unit quenchant-to-sphere temperature difference, are then calculated from the standard integrals, based on elastic theory (Timoshenko and Goodier 1951):

$$\left.\begin{aligned} {}_t\sigma_{(r,t)} &= \frac{E\alpha}{1-\mu}\left\{\frac{2}{R^3}\int_0^R \frac{T_{r,t}}{T_o}\, r^2 dr + \frac{1}{r^3}\int_0^r \frac{T_{r,t}}{T_o}\, r^2 dr - T_{r,t}\right\} \\ {}_r\sigma_{(r,t)} &= \frac{2E\alpha}{1-\mu}\left\{\frac{1}{R^3}\int_0^R \frac{T_{r,t}}{T_o}\, r^2 dr - \frac{1}{r^3}\int_0^r \frac{T_{r,t}}{T_o}\, r^2 dr\right\}, \end{aligned}\right\} \tag{16}$$

where E = elastic modulus

α = coefficient of thermal expansion

μ = Poisson's ratio

T_o = quenchant temperature.

The main features of this solution are that the temperature is uniquely determined by two parameters, Biot Number and a non-dimensional time modulus at/R^2. Thus, given a ball of known physical properties and dimensions, the temperature history may be computed provided the surface heat transfer coefficient is known. This normally requires a calibration of the test specimen, since heat transfer coefficient is dependent on geometry and quenchant properties. The most direct method would be to observe the temperature history during a typical quench and deduce the mean effective Biot Number by curve fitting. It may be an advantage to make the calibration on a sphere of high, accurately known and temperature insensitive thermal conductivity, such as Armco iron; Pryor and Rotsey (Unpublished) used this approach for a liquid metal quench experiment obtaining a calibration accuracy of 10-15 per cent. If a gas quenchant is being used, a steady state heat transfer measurement may be made, using a specially instrumented sphere, as developed by Lawther (1965). Dynamic similarity relationships may be applied so that the experiment may be made under more experimentally convenient conditions than those applying to the quench experiment; a calibration accuracy of better than 5 per cent. is obtainable. Using small heat flux meters, also developed by Lawther, the variation of local heat transfer coefficient may also be determined. This is a decided advantage if the heat transfer coefficient variation over the surface of the sphere is significant; the implications of this are discussed later.

Plots of non-dimensional surface tangential stress, $\left[{}_t\sigma_{(R,t)} \times \frac{(1-\mu)}{E\alpha}\right]$ versus time are shown in Figure 10 for two typical Biot Numbers. The smaller one, 1.5, would correspond to a high pressure gas quench of a 3.5 cm diameter BeO specimen and the higher one, 3.0, to a liquid metal quench of the same specimen. Figure 11 shows the non-dimensional mean and surface temperature histories

corresponding to those shown in Figure 10. Suppose the material under test has a value of 800 p.s.i./degC for the parameter $E\alpha/(1-\mu)$ (typical of beryllium oxide at 800 °C) and that it is required to generate a surface stress of 20,000 p.s.i. by quenching from 800 °C. Reference to Figures 10 and 11 provides the following quench amplitudes and surface and mean temperature at the instant of maximum stress:

TABLE 5

QUENCH AMPLITUDES AND TEMPERATURES OF TYPICAL SPECIMEN

Biot Number	1.5	3.0
Quench Amplitude	145 °C	95 °C
Surface Temperature	746 °C	753 °C
Mean Temperature	771 °C	779 °C

If the thermal conductivity of the material is temperature dependent, the question now arises as to the effect of this "non-ideal" behaviour on the accuracy of the predicted surface stress. The thermal conductivity of beryllium oxide, for instance, would be expected to increase by about 10 per cent. in cooling from 800 °C to 750 °C (Lillie 1961); reference to Figure 12, which graphs the variation of maximum surface stress with Biot Number, shows that this change of thermal conductivity could reduce the stress by about 6½ per cent. for both the high and low Biot Numbers considered here. So, unless this effect is allowed for, a maximum error of about 3 per cent. would be expected to arise in applying Carslaw and Jaeger's ideal model and choosing a material temperature between the pre-quench value and, say, the surface temperature at the instant of maximum stress. However, as indicated by Pryor and Rotsey (Unpublished), this error can be eliminated by applying a finite difference analysis using a differential equation computer code on the lines of that developed by Bennett (1965).

Another important assumption in Carslaw and Jaeger's analysis is that of uniform heat transfer over the surface of the sphere. If the heat removal during the quench is by conduction only, and the quench bath is large with respect to the specimen, this assumption will be valid. However, there will always be a convection component, even in a liquid metal quench bath the specimen has to be lowered into it and a flow disturbance will remain after the specimen comes to rest. As soon as a convection component is introduced, the heat transfer ceases to be uniform because of variations in fluid velocity around the sphere. Rotsey and Pryor (Unpublished) have estimated that this non-uniformity could cause local thermal stress increases of about 10 per cent. for quenches in liquid metal. Using an analysis by Thompson (1965), Holy (Unpublished) has shown that an increase as high as 30 per cent. could be obtained with heat removal entirely by convection, as would be the case in a gas quench. Therefore in any quench experiment, significant errors could arise.

Two approaches are available to nullify or account for this error. Either the surface heat removal under service conditions can be simulated in the test so that its effect is "built-in" and need not be known, or the surface heat transfer variation under test conditions is measured and allowed for in the translation of the test results into an in-service failure criterion. Practical difficulties would almost preclude experimental measurement of local heat transfer with liquid metal quenchant; measurements with gas quenchant are feasible and have been successfully obtained, as mentioned above. Of the alternatives of either "building in" the service conditions of local heat transfer variation or accepting the measured experimental values and accounting for the non-simulation by analysis, the former is to be preferred, because of the complexity of the calculations. Departures from the simplifying condition of axial symmetry require an increase of already significant computer effort. The A.A.E.C. gas quench rig, at present under construction, closely simulates the in-service flow conditions, at the expense of a slight increase in the size and complexity of the apparatus.

4.2 Multiple Specimens

The temperature history of the quenchant, in its passage through a multiple specimen, can be derived from heat regenerator theory. Schumann (1929) for instance, derived an analytical solution for the case of incompressible flow through a uniform storage medium, whose thermal conductivity is

treated as infinite and the physical and thermodynamic properties as uniform. In the present context, the thermal conductivity cannot be assumed infinite and a new solution has therefore been derived. Such a solution is absent from the literature because most engineering applications conform to the assumptions of Schumann's analysis. The approach has been part analytical, part numerical; as a first approximation, Schumann's solution is assumed and successive approximations are then obtained by carrying out a heat balance between the temperature rise of the quenchant and the temperature drop of the specimen.

The regenerator is treated as an array of identical spheres distributed at uniform voidage; an ordered array would conform to this condition. Longitudinal conduction of heat is considered negligible with respect to the heat removed by convection. This is considered reasonable in view of the high thermal resistance offered by the point contacts on the spheres and the flow velocities of the quenchant – of the order of tens of feet per second. Non–ideal behaviour will be caused by local regions of non–uniform velocity and turbulent mixing, resulting in a distortion of the nominally uniform temperature distribution across the array. This would be difficult to account for in the analysis and has been neglected; however, the array would be calibrated in order to obtain the test value of heat transfer coefficient (and hence Biot Number) and such a departure from ideal behaviour would be absorbed in the measured value. To summarise, the assumptions are:

1. The regenerator consists of identical spheres distributed at uniform voidage.
2. The sphere material density, specific heat, thermal conductivity, Young's Modulus, coefficient of thermal expansion, and Poisson's Ratio are constant over the temperature range of the quench.
3. The sphere surface heat transfer coefficient is uniform throughout the bed and during the quench.
4. Elastic theory applies to the calculation of thermal stress.
5. The quenchant is an incompressible fluid of zero thermal conductivity.
6. Quenchant velocity distribution is uniform throughout the regenerator.
7. The only transfer of heat is that between the quenchant and the spheres.
8. The approach conditions of the quenchant are constant during the quench.
9. Initial temperature of the regenerator is zero and the temperature of the quenchant entering the regenerator is constant.

The system is fully described by the following three differential equations:

(a) Conduction equation of a sphere, spherical symmetry:

$$\frac{1}{r}\left\{2\frac{\partial T_r}{\partial r} + r\frac{\partial^2 T_r}{\partial r^2}\right\} = \frac{1}{a}\frac{\partial T_r}{\partial t} \quad . \tag{17}$$

(b) Conduction heat flux at ball surface equal to heat transferred to gas:

$$k\left(\frac{\partial T_r}{\partial r}\right)_R = h\,(T_g - T_R) \quad . \tag{18}$$

(c) Heat balance between the conduction heat flux at the surface of the ball and the enthalpy rise of the gas:

$$\frac{-3k(1-V)}{C_p R}\left(\frac{\partial T_r}{\partial r}\right)_R = W\frac{\partial T_g}{\partial x} + \rho V\frac{\partial T_g}{\partial t} \quad , \tag{19}$$

With the following boundary conditions

$$T_r = 0, \quad t \leq 0, \quad R \geq r \geq 0, \quad x > 0$$

$$T_g = T_q \text{ at } x = 0 ,$$

and where
- T = temperature
- r = radial position in sphere
- a = thermal diffusivity of the sphere material
- t = time, measured from time of arrival of quench front at position of interest
- k = thermal conductivity of the sphere material
- h = surface heat transfer coefficient of sphere
- V = regenerator voidage
- R = sphere radius
- W = quenchant mass flow per unit cross-sectional area
- x = distance downstream of regenerator entry
- ρ = quenchant density
- C_p = quenchant specific heat
- BN Biot Number ,

and suffixes are

- R = at radial position R on sphere, that is, the surface
- r = at radial position r in sphere
- g = quenchant, in regenerator
- q = quenchant, at regenerator entry
- x = distance downstream of regenerator entry .

These symbols are consistent with those used elsewhere in the paper.

A further boundary condition is given by:

$$(T_g)_{x,\, t=o} = T_q \exp\left(\frac{-3x.BN.k.(1-V)}{R^2.\, Cp.\, W}\right) .$$

A solution for T_r is required so that the tangential and radial stresses may be obtained by integration on the lines of Equation 18. Let the solution be of the form

$$T = A(t).\ G(r) , \qquad (20)$$

where A(t) and G(r) are respectively functions of time only and radial position only.

Substituting in Equation 17, it may be shown that:

$$\frac{1}{r} 2 \frac{dG(r)}{dr} + r \frac{d^2 G(r)}{dr^2} + \lambda^2 G(r) = 0 \quad , \tag{21}$$

where λ is a constant.

A solution of (21) is: $G(r) = g . \frac{\sin \lambda r}{r}$, (22)

where g is a constant.

λ may be evaluated by substituting for T in Equation A2 (See Appendix) giving:

$$k \left[\frac{dG(r)}{dr}\right]_R + hG(r) = \frac{hT_g}{A(t)} \tag{23}$$

Since the variables are separable, both sides of this equation are equal to a constant, which, by considering the boundary condition $T_r = \frac{\partial T_r}{\partial r} = 0$ when $t = 0$, may be seen to be zero.

$$\text{Thus } k \left[\frac{\partial G(r)}{\partial r}\right]_R + hG(r) = 0 \quad , \tag{24}$$

and the following solution for λ is obtained:

$$\left(\frac{hr}{k} - 1\right) = -R\lambda \cot R\lambda \quad .$$

The term $\frac{hR}{k}$ is the Biot Number, defined in Section 4.1.

Of the infinite number of solutions for λ, the first six are tabulated by Carslaw and Jaeger.

A property of the above solution is:

$$\int_0^R r^2 G_i(r) G_j(r) dr = 0 \quad \text{if } i \neq j \tag{25}$$

which may be normalised to give

$$\int_0^R r^2 G_i(r) G_j(r) dr = 1 \quad \text{if } i \neq j \quad ,$$

where the suffixes i and j refer to the i^{th} and j^{th} roots of the solution.

Expressing A(t) as a polynomial, T_r may therefore be written:

$$T_r = \sum_{i=1}^{\infty} A_i(t) G_i(r) \quad .$$

Multiplying both sides by $G_j(r)$ and integrating over the volume of the ball gives:

$$\left.\begin{aligned} \int_0^R T_r G_j(r) dr &= \int_0^R r^2 G_j(r) . \sum_{i=1}^{\infty} A_i(t) . G_i(r) dr \\ &= \dot{A}_j(t) \text{ from the property given by Equation 25.} \end{aligned}\right\} \tag{26}$$

The property given by Equation 25 may also be exploited to show that:

$$g_i^2 = \frac{2}{R - \frac{\sin 2\lambda_i R}{2\lambda_i}} \quad . \tag{27}$$

$A_i(t)$ is, as yet, not explicitly defined, since Equation 26 is also in T. By multiplying both sides of Equation 17 by $G_i(r)$ and integrating over the volume of the ball, the following is obtained:

$$\left[r.\, G_i(r) \frac{d}{dr}(r.\, T_r)\right]_0^R - \left[r.\, T_r \frac{d}{dr}(r.\, G_i(r))\right]_0^R + \int_0^R r\, T_r \frac{d^2}{dr^2}(r.\, G_i(r))\, dr \quad ,$$

$$= \frac{1}{a} \frac{dA_i(t)}{dt} \quad .$$

The terms in $\frac{dG_i.(r)}{dr}$, T_r, and $\frac{dT_r}{dr}$ may be eliminated by substituting from Equations 18, 24, and 21, thus:

$$\frac{R^2 h}{k} . G_i(r) T_g - \lambda_i^2 A_i(t) = \frac{1}{a} \frac{dA_i(t)}{dt} \quad . \tag{28}$$

Integrating from 0 to τ and noting that $A_i(0) = 0$, the following is obtained:

$$A_i(\tau) = \frac{ak^2 h\, G_i(R)}{k} \int_0^\tau T_g \exp\{-a\lambda_i^2 (\tau - t)\}\, dt, \text{ which is the explicit form required.}$$

Thus, by definition, $T_r = \sum_{i=1}^{\infty} A_i(t)\, G_i(r)$,

$$= \sum_{i=1}^{\infty} \frac{aR^2 h}{k} G_i(R).G_i(r) \int_0^\tau T_g \exp\{-a\lambda_i^2 (\tau - t)\}\, dt \quad . \tag{29}$$

A solution for T_g must now be obtained.

By appropriate substitution in the heat balance Equation 19, the following differential equation in T_g is obtained:

$$W\left(\frac{\partial T_g}{\partial x}\right)_\tau + \rho V\left(\frac{\partial T_g}{\partial t}\right)_\tau = \frac{3a\, Rh^2 (1-V)}{C_p k} \sum_{i=1}^{\infty} [G_i(R)]^2 \int_0^\tau T_g \exp\{-a\lambda_i^2 (\tau - t)\}\, dt \quad (30) .$$

The problem has now been broken down to two separate problems; firstly, to evaluate T_g from Equation 30, and, then secondly, to evaluate T_r from Equation 29. Equation 30 was solved by a finite difference method. The development of a convergent solution proved to be difficult; an outline of a successful approach is given in the Appendix.

It transpires that the Biot Number grouping is also one of the independent non-dimensional variables in the finite thermal conductivity regenerator solution; reference to the Appendix will show that the thermodynamic capacities of the quenchant and the storage medium are also independent variables. It is therefore impracticable to generate generalised data for this analysis, as is possible for the isolated sphere case. Interest therefore centres on what is considered a typical set of conditions that would apply to a quench test of 3.5 cm diameter ceramic spheres at 800 °C, using pressurised carbon dioxide as quenchant. A typical value of 1.5 will be chosen for the Biot Number for what will be referred to as the standard case. The assumed physical and thermodynamic properties of the quenchant and specimen will be as follows:

Specimen:	Thermal Conductivity.	0.1 cal/deg C. sec. cm
	Density	2.5 g/cm^3
	Specific Heat	0.2 cal/g. deg C
	Voidage in Specimen Assembly	0.4
Quenchant:	Density	0.01 g/cm^3
	Specific Heat	0.3 cal/g. deg C
	Mass Flow/Unit Area	10 $g/sec. cm^2$.

A typical specimen geometry would be an array of spheres of total cross–section 7 ball diameters square and a depth of 10 to 15 diameters, giving a sample size of about 300–400, allowing for voidage. The sample would be inspected after quenching by taking it to pieces, ball by ball, and inspecting for surface cracks; the longitudinal position of a particular ball would have to be noted in order to obtain the quenchant temperature and thus stress history at that point in the array. A development of this may be to cast the whole array in epoxy resin after quenching and inspect machined lateral slices for cracks.

Figure 13 shows gas temperature histories at two points along the specimen; 25 and 50 cm from the upstream face. Also included are the corresponding histories given by Schumann's solution. The difference between the two solutions is significant, particularly in the initial period of the quench. The stress history of the specimen is summarised in Figure 14. Figure 15 is a cross plot of the maximum stress versus distance along the specimen; also shown is the cross plot corresponding to the gas temperature history given by Schumann's solution. These results show, firstly, that accounting for the finite thermal conductivity of the specimen in the calculation of gas temperature history was justified, because the maximum stress is affected by about 10 per cent. by so doing. Secondly, a statistically sufficient wide stress spectrum can be obtained from a single quench of the multiple specimen; for instance, the amplitude of the quench can be set so that the mean stress is expected to occur at, say, 20 cm from the upstream face. There would be available a range of stress either side of the mean value to accommodate 1 to 2 standard deviations above and below the mean, given standard deviations of 10 to 15 per cent. of the mean. There would also be available some "spare" specimen to account for a poor guess of the mean prior to the test, so that the desired symmetry of the stress levels about the mean could be maintained.

As is the case for the single specimen, the multiple specimen has to be calibrated in order to know the test Biot Number. It would normally be impracticable to apply steady state methods, because of the size of the specimen, and a transient method would therefore have to be used. In order to reduce the speed of temperature response of the specimen (to ease instrumentation difficulties) and to reduce temperature gradients within the individual sphere, a replica specimen of copper or Armco balls could be used for calibration purposes. Keeping all other conditions the same as the standard case, the Biot Number would be about 0.15 for a copper specimen, and ball temperature histories of the type shown on Figure 16 would be obtained. An adequately measurable temperature change would be obtained from a quench amplitude of 200 °C, and a thermocouple time constant of about 10 milliseconds would be sufficiently short to enable the change to be followed with negligible lag errors. If heat transfer coefficient varies along the specimen due to flow entry effects, the quenchant temperature history must also be recorded. The ball temperature histories at each point would then have to be curve fitted to predicted histories appropriate to the assumed Biot Number and temperature history. The finite–difference analysis described in the Appendix can be adapted to this calculation.

The only quenchant property to be affected significantly by the temperature changes of interest is density. Since it is the product of density and fluid velocity that determines the rate of heat removal in forced convection, changes of density would not be expected to have any effect on thermal stress provided no re–distribution of flow through the specimen took place. This has been confirmed by calculation. The error introduced by changes of specimen thermal conductivity with temperature is

of the same order as for the isolated sphere and the approach to accounting for these errors is the same, with the added complication of a time varying quenchant temperature. Bennett's computer code (Bennett 1965) could be successfully applied to such an analysis.

The approach to the problem of non–uniform heat transfer over the surface of the ball would correspond to the first of the two alternatives proposed in the previous section, that is, it would be treated as a "built–in" effect. This approach would be applicable to orderly or random packing of the spheres in the test specimen, which would replicate the packing expected in service.

4.3 Validity and Accuracy of the Quench Technique

Provided effects of strain rate and stress relaxation are unimportant, the only validity criterion that can be applied is that of similarity of temperature distributions (and hence thermal stress) in the test and in service. Although the effect of the temperature dependence of thermal conductivity can be accounted for, there remains the possibility that any significant difference in the temperature distribution could have an effect on the mode of failure of the ball. The failure could vary between the two extremes of surface crazing and complete disintegration. Figure 17 compares the temperature distributions at the instant of maximum stress for single and multiple specimens to those of a sphere having uniform internal heat generation in the steady state, characteristic of a nuclear reactor application. The comparison is encouraging; from the surface to a depth of about 0.2 (radius) below the surface, the temperature distributions, expressed as a change from the pre–quench condition, agree to within 10 per cent. The surface heat fluxes and temperatures for the quench and steady state conditions were equalised for this comparison. The significance of the temperature distribution at greater depths decreases because failure is expected to occur at the surface, and the stress integral is decreasingly sensitive to temperatures as the centre of the ball is approached (Equations 16).

A full analysis of the accuracy of the estimate of thermal stress resistance obtainable from quench testing is outside the scope of this paper. Furthermore, the accuracy depends on many details of experimental technique which would vary between laboratories. Unpublished estimates applicable to techniques in use at the A.A.E.C. Research Establishment have shown that an accuracy of $\pm 5 - 10$ per cent. should be readily attainable.

5. CONCLUSIONS

1. Low in–service failure rates, within the range 1/1000 to 10/1000, impose stringent accuracy requirements on the specification of a working stress of materials such as ceramics, which exhibit significant scatter in failure stress. The accuracy required is determined by the tolerance available on failure rate. (Figures 1 and 2 summarise the interchange between these two variables for a typical case).

2. The statistical model of the probability distribution of failure stress has a significant effect on the accuracy and sample size requirements of a quench testing programme.

3. Determination of working stress by quench testing has to be approached statistically using the Quantal Response or Up–and–Down methods. Both these methods exhibit bias in the deduced value of working stress. This bias can be accounted for (Figure 3).

4. Estimates of accuracy, calculated from many sets of simulated quench data, can be summarised in a way that enables predictions to be made of accuracy or sample size required for a given experiment (See for example, Figures 8 and 9). In general, sample sizes are of the order of hundreds.

5. The Up–and–Down Method requires between half and two–thirds the sample sizes of the Quantal Response Method.

6. The accuracy of the Quantal Response Method can be adversely affected by a poor initial guess of the mean, because of the resulting asymmetric distribution of the stress levels about the mean. This may be overcome by an initial test on a small sample of about 40 specimens using the Up–and–Down Method to obtain a better guess of the mean.

7. The accuracies of the Quantal Response and the Up–and–Down Methods appear to be insensitive to poor initial guesses of the standard deviation, provided the guess is on the high side.

8. The thermodynamics of single specimen quenching is well established and is amenable to application as a test technique.

9. The thermodynamics of multiple specimen quenching has been analysed as a heat regenerator problem. The additional complexity of the finite thermal conductivity solution is justified by the error that would be obtained with Schumann's infinite thermal conductivity solution.

10. The range of thermal stress obtainable from a single quench of a multiple specimen is sufficiently wide for a value of design thermal stress to be deduced from the results of a single test.

11. Both single and multiple specimen quench experiments require a calibration in order to establish the test value of surface heat transfer coefficient.

12. The validity and accuracy of the quench technique as applied to the derivation of thermal stress resistance are considered adequate.

6. ACKNOWLEDGEMENTS

Grateful acknowledgement is made to Mr. E. Szomanski, Section Head, Experimental Research and Development Section, A.A.E.C. Research Establishment, for discussions and encouragement in the work involved in producing this paper, Professor J.J. Thompson, of the University of N.S.W., for the derivation of the analytical part of the heat regenerator solution, and Mr. J.F. Whatham, A.A.E.C., for Figure 12, which was transcribed from an internal A.A.E.C. report.

7. REFERENCES

Bennett, N.W. (1965). – DEMON – A programme generator for problems involving ordinary differential equations. AAEC/E142.

Carslaw, H.S., Jaeger, J.C. (1959). – Conduction of Heat in Solids. Clarendon Press, Oxford.

Dixon, W.J., Mood, A.M. (1948). – A method for obtaining and analysing sensitivity data. Journal of the American Statistical Assoc., 43 : 109–126.

Finney, D.J. (1962). – Probit Analysis. Cambridge University Press, Cambridge, 1962.

Fisher, Sir Ronald, Yates, F.A. (1957). – Statistical Tables for Biological, Agricultural and Medical Research. Oliver and Boyd, London.

Lawther, K.R. (1965). – Development of an experimental technique for measuring local heat transfer from a sphere. The 2nd Australasian Conference on Hydraulics and Fluid Mechanics, December, 1965.

Lillie, J. (1961). – Some properties of beryllium oxide, UCRL 6457.

Paradine, C.G., Rivett, B.H.P. (1964). – Statistical Methods for Technologists. English Universities Press, London.

Roberts, W.H. (1964). – The Australian high temperature gas cooled feasibility study. J. Nucl. Mat. 14 : 29–40 .

Schumann, T.E.W. (1929). – Heat transfer : a liquid flowing through a porous prism. Journal of the Franklin Institute, 208, 1245–29.

Thompson, J.J. (1965). – Thermoelastic stresses in a homogeneous spherical fuel element of a pebble bed reactor, AAEC/TM285.

Timoshenko, S., Goodier, J.N. (1951). – Theory of Elasticity, McGraw Hill.

Whitaker, Sir Edmund, Robinson, G. (1962). – The Calculus of Observations. Blackie & Sons, London.

Wright, W.J. (1964). – Methods and costs of refabrication in relation to performance of beryllia in an H.T.G.C. reactor, J. Nucl. Mat. 14 : 349–358.

APPENDIX

FINITE DIFFERENCE SOLUTION OF THE FINITE THERMAL CONDUCTIVITY HEAT REGENERATOR PROBLEM, GIVEN A NON-CLOSED ANALYTICAL SOLUTION IN INTEGRAL FORM

Firstly, Equation 19 is replaced by the heat balance between the sphere and the gas:

$$W \frac{\partial T_g}{\partial x} + \rho V \frac{\partial T_g}{\partial t} = - \frac{Cp_b}{Cp} \rho_b (1 - V) \frac{\partial \bar{T}_b}{\partial t} \quad , \qquad (A1)$$

where Cp_b = specific heat of ball

ρ_b = density of ball

$\bar{T}_b$ = mean temperature of the ball

$$= \frac{3}{R^3} \int_0^R T_r \, r^2 \, dr \quad .$$

Substituting for T_r from Equation 29:

$$\bar{T}_b = \sum_{i=1}^{\infty} \frac{aR^2h}{k} G_i (R) \int_0^{\tau} T_g \exp \{ - a\lambda_i^2 (\tau - t) \} dt \times \frac{3}{R^3} \int_0^R r^2 G_i (r) dr ,$$

$$= 3 \sqrt{\frac{2aRh}{Rk}} \sum_{i=1}^{\infty} G_i (R) \frac{\left(\frac{\sin \lambda_i R}{\lambda_i R} - \cos \lambda_i R \right)}{(R\lambda_i)^2 \sqrt{1 - \frac{\sin 2\lambda_i R}{2\lambda_i R}}} \times \int_0^T T_g \exp \{ - a\lambda_i^2 (\tau - t) \} dt . \qquad (A2)$$

Secondly, the integral occurring in Equations 29 and A2 can be expanded in finite difference form as follows:

$$\int_0^{\tau} T_g \exp \{ - a\lambda_i^2 (\tau - t) \} dt = \sum_{j=0}^{m-1} \int_{j.\delta t}^{(j+1)\delta t} \left[T_g (n,j) + \left\{ \left(\frac{T_g (n,j+1) - T_g (n,j)}{\delta t} \right) (t - j\delta t) \right\} \right] \times$$

$$\times \exp \{ - a\lambda_i^2 (\tau - t) \} dt \quad ,$$

where $m = \frac{\tau}{\delta t}$ and $T_g (n,m)$ is the gas temperature at the n^{th} distance interval down the regenerator after expiration of m time intervals from the start of the quench at that position. The integral may now be expanded in the normal way.

Thirdly, the finite difference increment may be specified:

$$\delta x = \frac{W \delta t}{\rho V K} \quad ,$$

where K is an arbitrary factor determined by the geometry of the problem. Thus Equation A1 may now be written in finite difference form:

$$T_g(n,m+1) - T_g(n,m-1) + K \left(T_g (n+1,m) - T_g (n-1,m) \right) - \frac{1}{2} \left(T_g (n+1,m+1) - T_g (n+1,m-1) + T_g (n-1,m+1) - T_g (n-1,m-1) \right)$$

$$= \frac{Cp_b}{Cp} \cdot \frac{\rho_b}{\rho} \frac{(1 - V)}{V} \left(\bar{T}_b (n,m-1) - \bar{T}_b (n,m+1) \right) \qquad (A3)$$

or DELT (n,m) = DELB (n,m), say.

(continued)

APPENDIX (continued)

For an incorrect first approximation $T_g(n,m)$ an error term $E(n,m)$ may be calculated:
$E(n,m) = DELB(n,m) - DELT(n,m)$. and a correction to T_g may then be found:

$$\Delta T\ (n,m) = \frac{1}{K-1}\ \Big[E(n-1,m) - \Delta T_g\ (n-1,m+1) + \Delta T_g\ (n-1,m-1) + K\Delta T_g(n-2,m)$$
$$- \Delta T_g\ (n,m-1) + \frac{1}{2}\ (\Delta T_g(n-2,m+1) - \Delta T_g(n-2,m-1))\Big] \quad , \qquad (A4)$$

By evaluating $\Delta T_g\ (n,m)$ in the order of ascending m and n, and making appropriate adjustments on the boundaries, the whole finite difference mesh can be covered, except that the maximum value of m is reduced by 1 for each distance step.

The second approximation may then be calculated

$$T_g(n,m) = T_g\ (n,m) + \Delta T_g\ (n,m) \quad , \qquad (A5)$$

and the process repeated.

It was found that some damping of the correction was necessary in order to obtain a non-oscillatory solution, that is,

$$T_g(n,m) = T_g\ (n,m) + D\Delta T_g\ (n,m) \quad ,$$

where $0 < D \leqslant 1$. For the results quoted in this paper, D was set at 1/2 and about 12 approximations were necessary to obtain a solution to within 0.1 per cent. of its asymptotic value.

Given the value $T_g\ (n,m)$ throughout the regenerator, the corresponding values of $T_r(n,m)$ may now be found, and the stresses calculated according to Equation 16 of the main text.

By expanding Equation A2, it may be shown that the constant term outside the summation may be arranged as a function of two non-dimensional groupings: Biot Number, $\frac{hR}{k}$, and "Incremental Time Modulus", $\frac{\delta ta}{R^2}$.

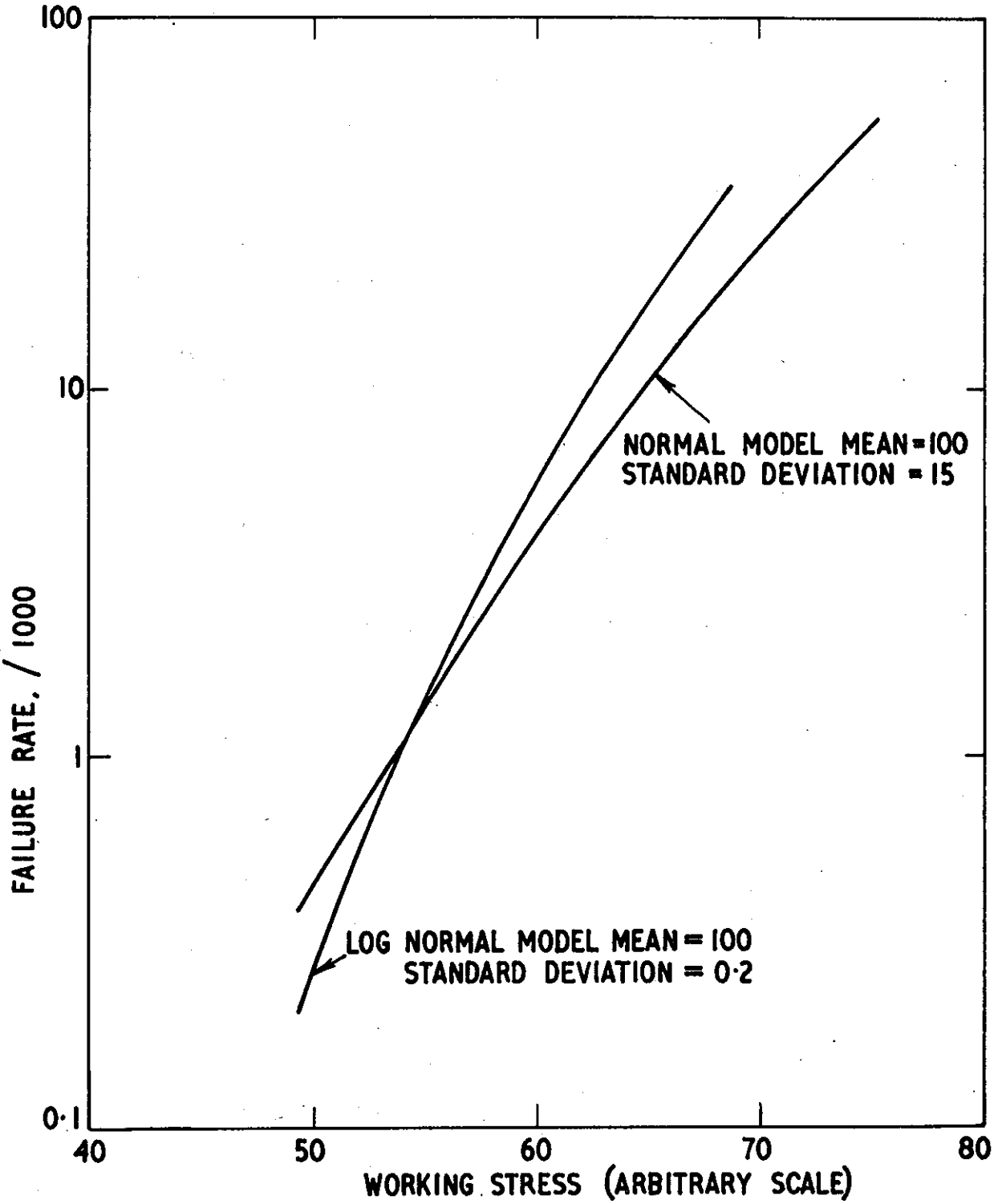

FIGURE 1. VARIATION OF FAILURE RATE WITH WORKING STRESS FOR LINEAR NORMAL AND LOG NORMAL MODELS

P. 1026

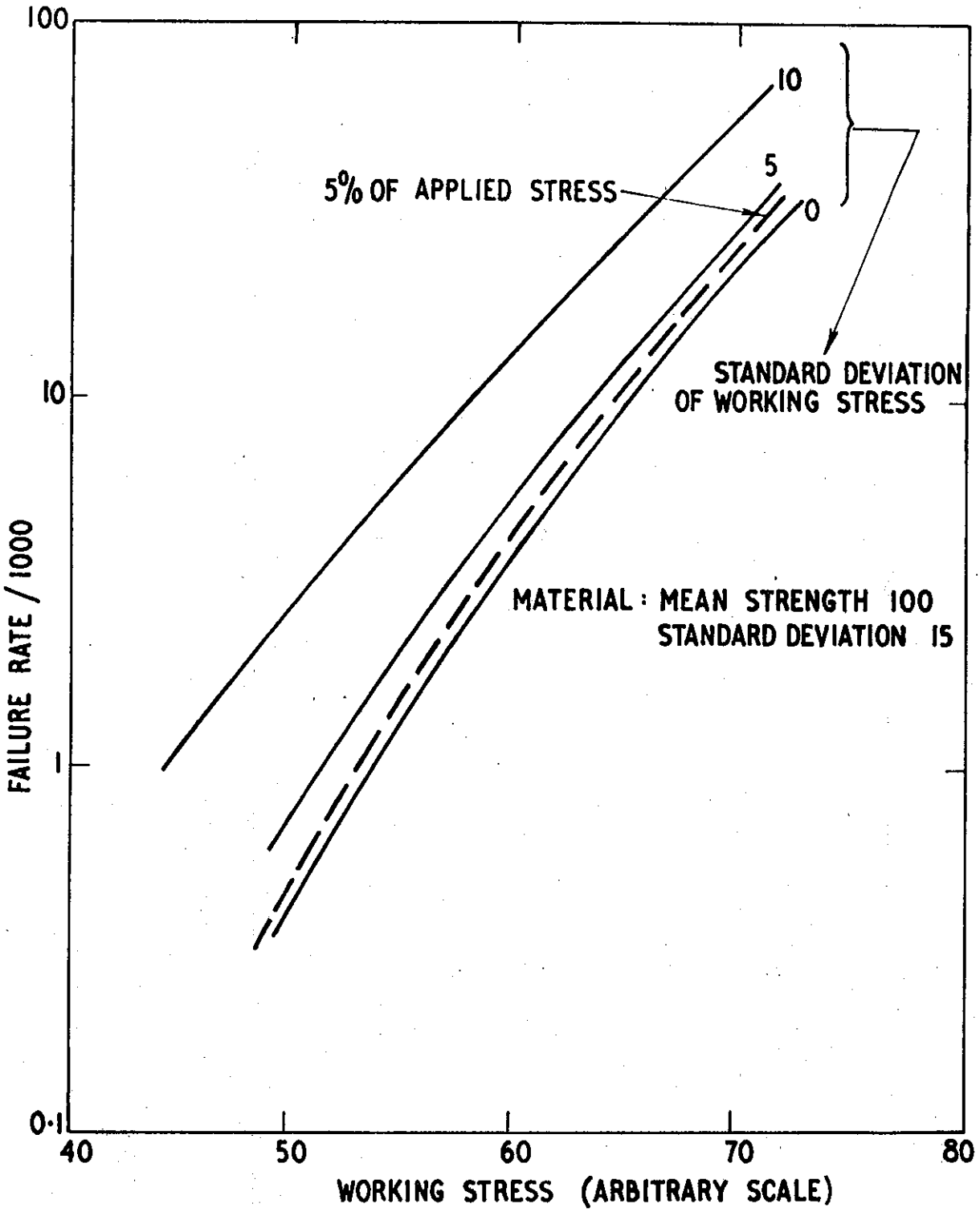

FIGURE 2. EFFECT OF WORKING STRESS DISTRIBUTION ON FAILURE RATE FOR LINEAR NORMAL MODEL

P1026

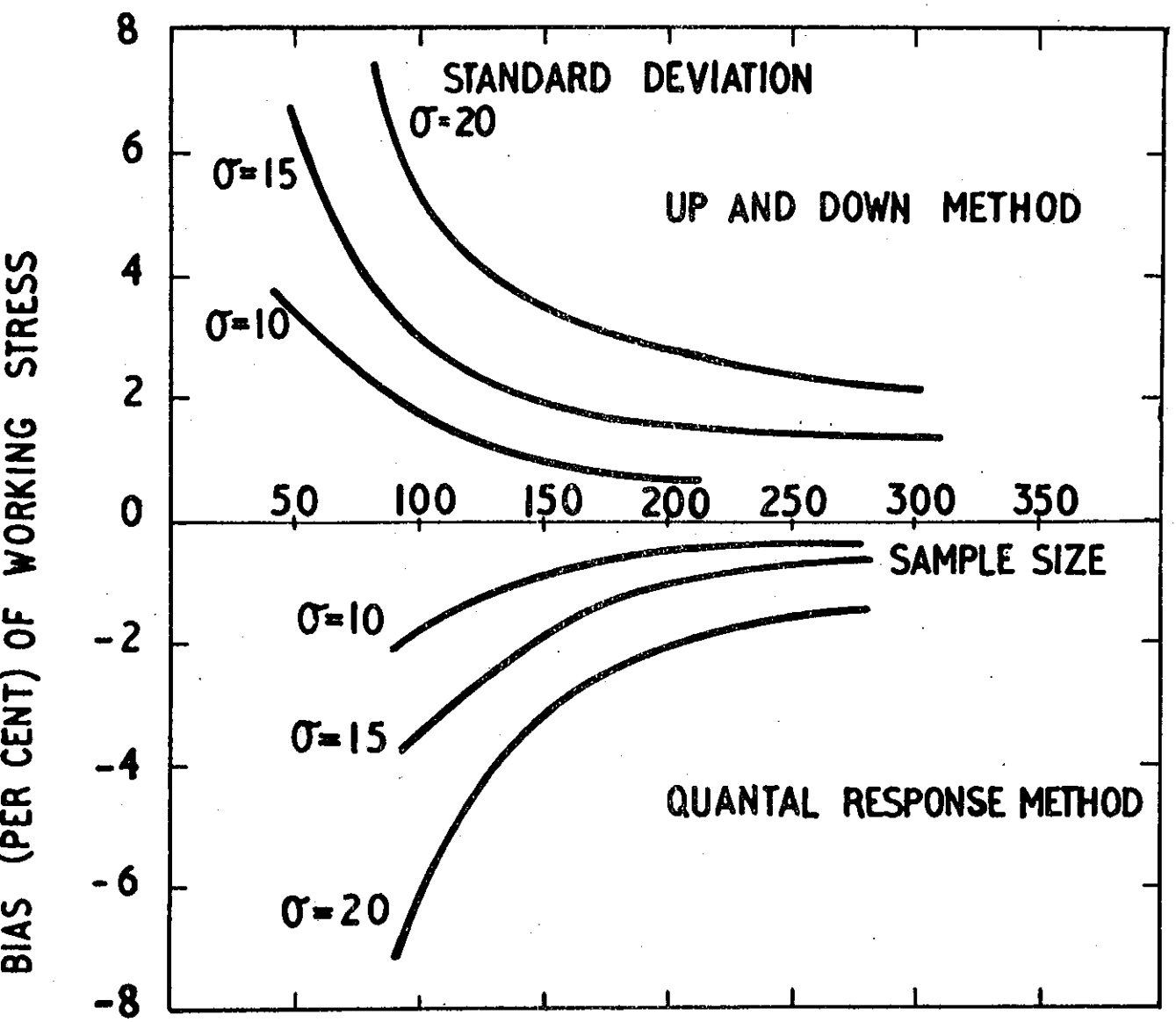

IGURE 3. VARIATION OF BIAS WITH SAMPLE SIZE, LOW FAILURE RATE, LINEAR NORMAL MODEL

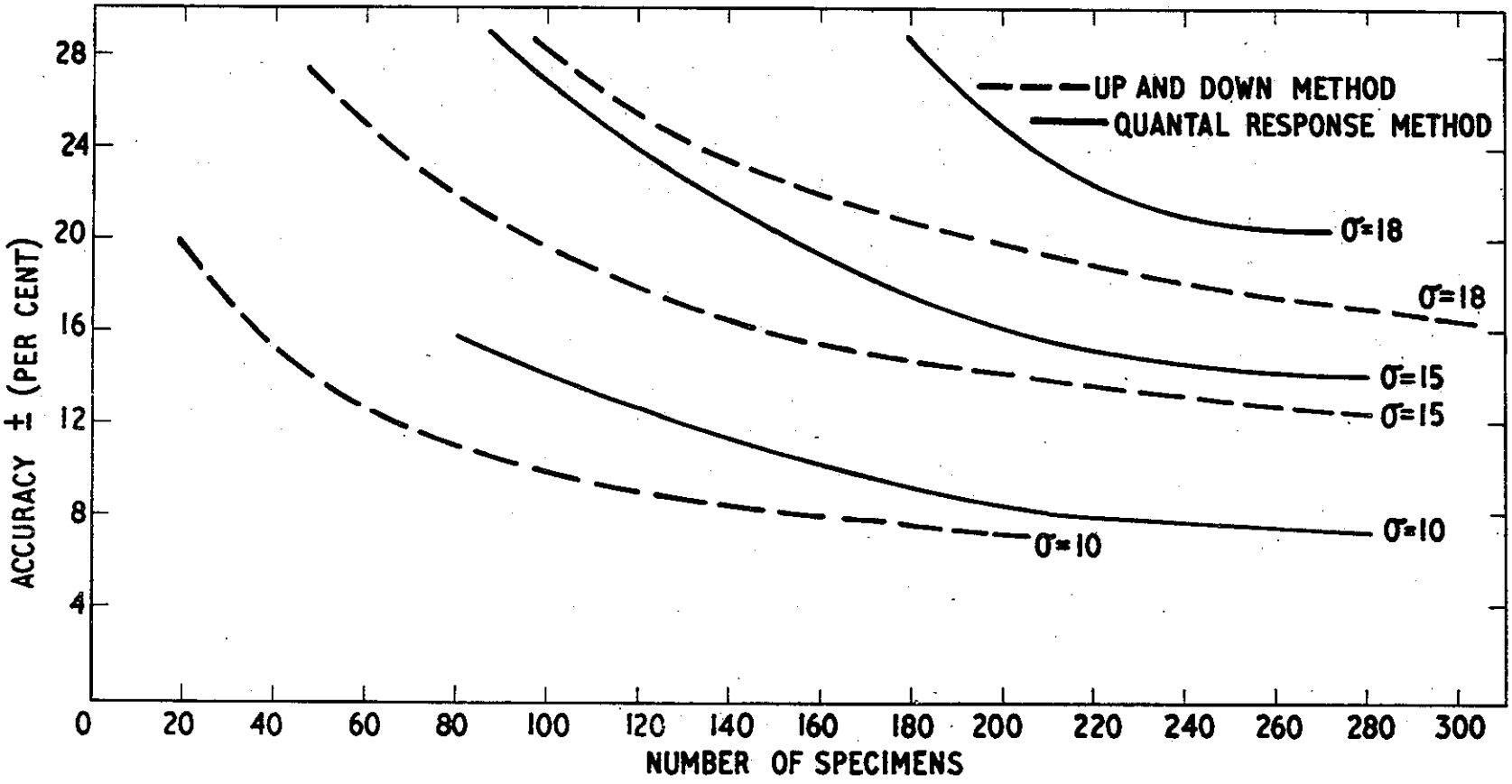

FIGURE 4. VARIATION OF ACCURACY OF DEDUCED WORKING STRESS WITH SAMPLE SIZE, LINEAR NORMAL MODEL, LOW FAILURE RATE

P1026

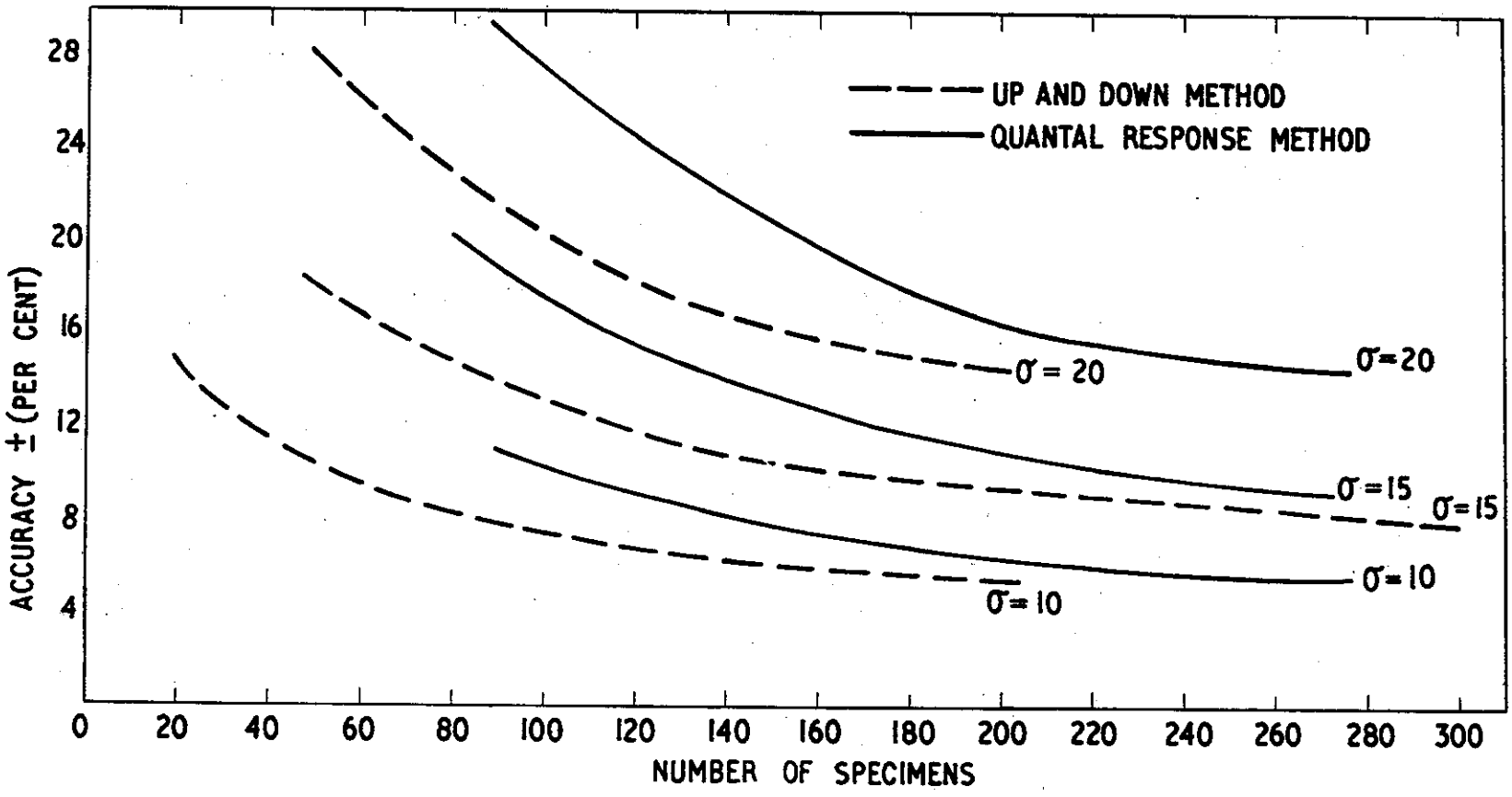

FIGURE 5. VARIATION OF ACCURACY OF DEDUCED WORKING STRESS WITH SAMPLE SIZE, LINEAR NORMAL METHOD, HIGH FAILURE RATE

P1026

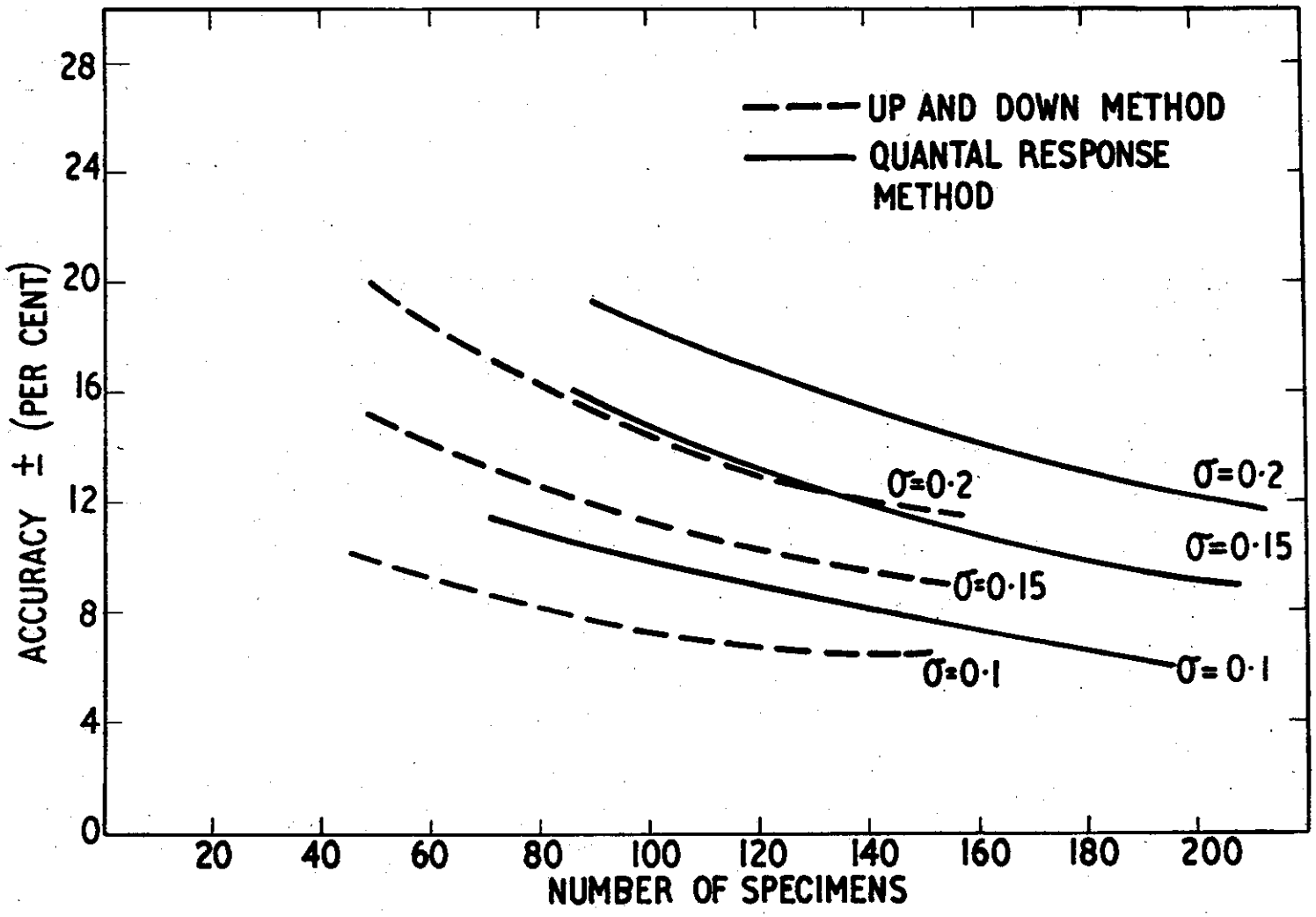

FIGURE 6. VARIATION OF ACCURACY OF DEDUCED STRESS WITH SAMPLE SIZE, LOG NORMAL MODEL, LOW FAILURE RATE

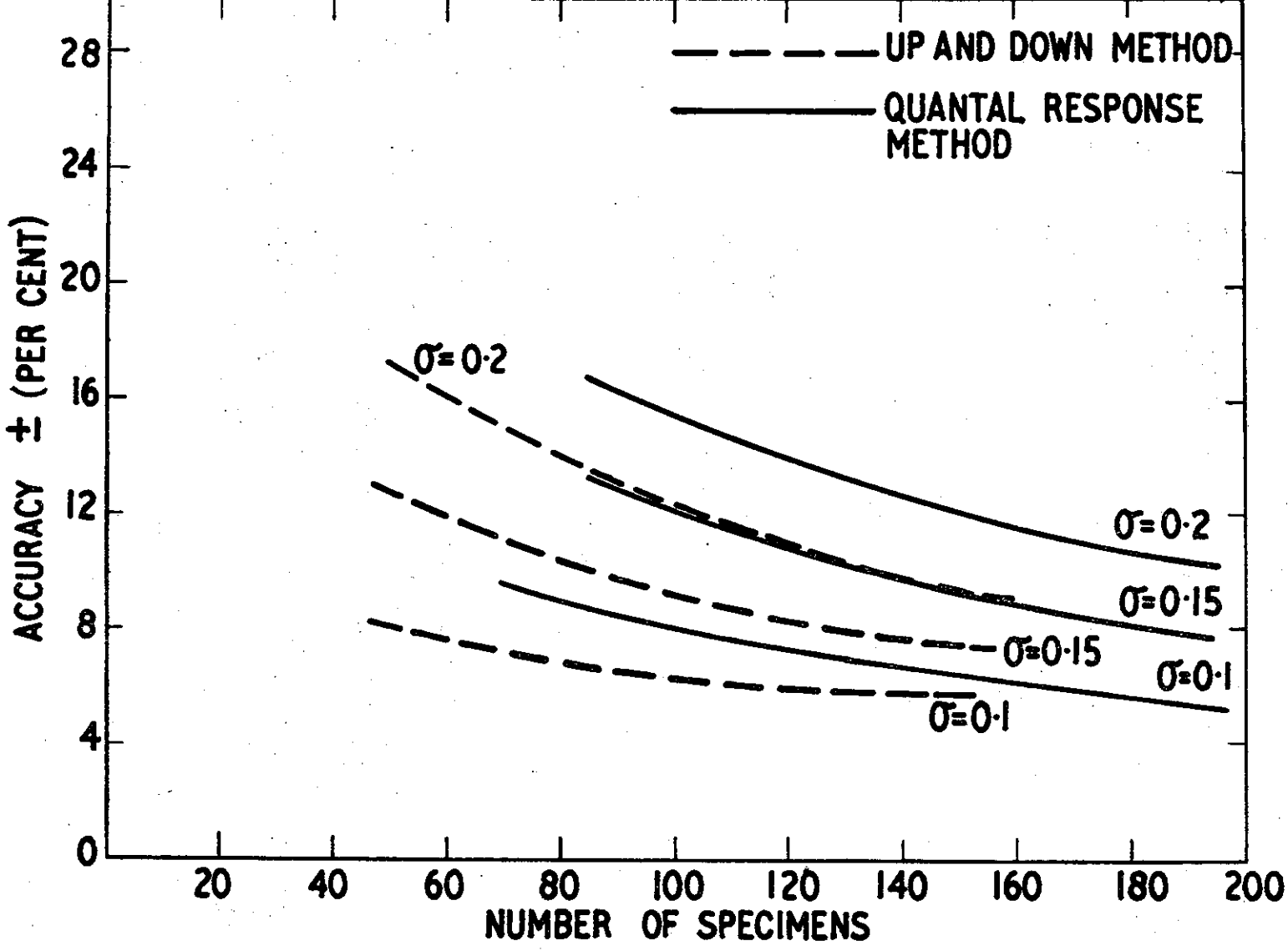

FIGURE 7. VARIATION OF ACCURACY OF DEDUCED STRESS WITH SAMPLE SIZE, LOG NORMAL MODEL, HIGH FAILURE RATE

P 1026

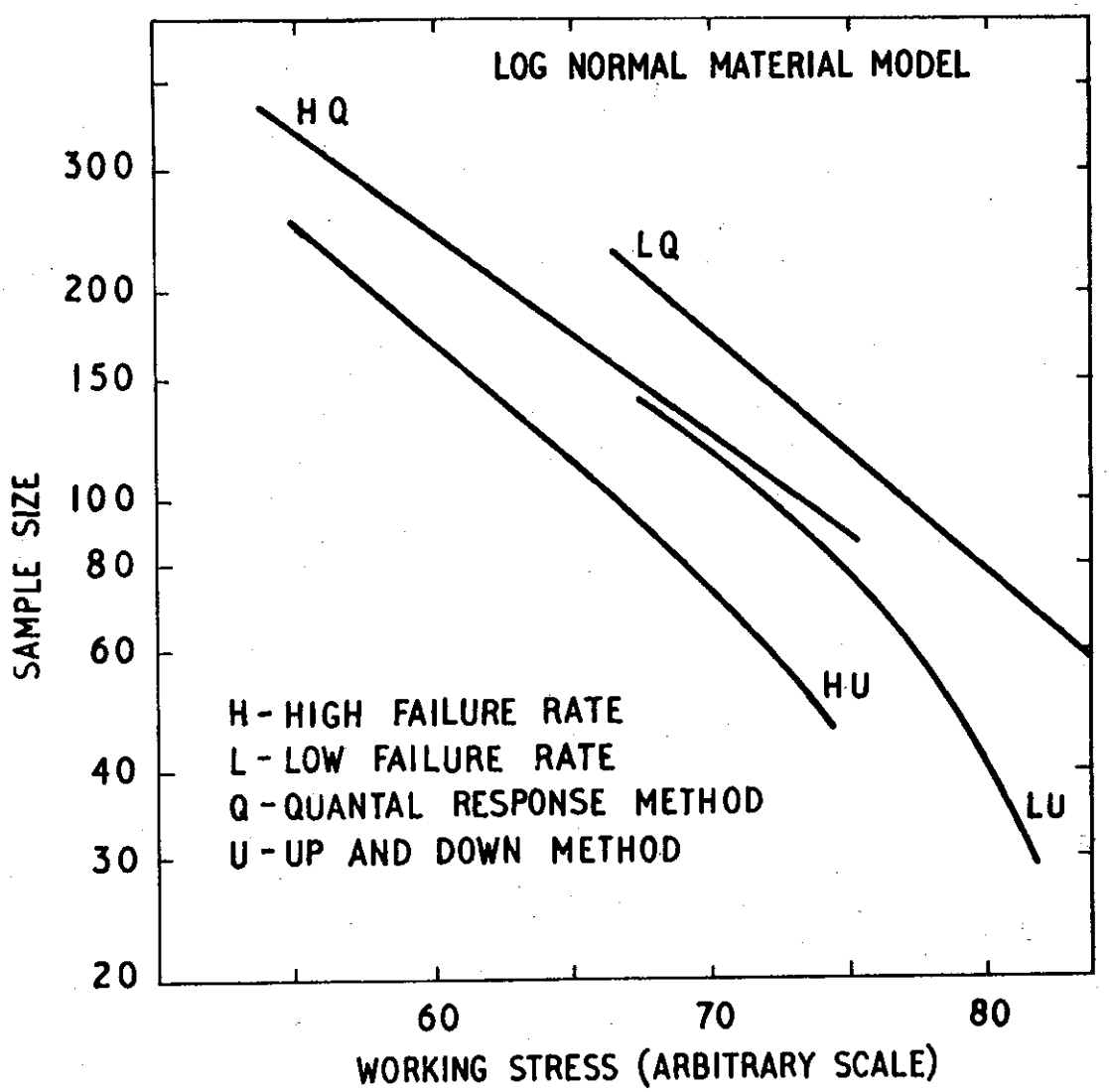

FIGURE 8. VARIATION OF SAMPLE SIZE REQUIRED TO OBTAIN A WORKING STRESS ACCURACY ± 10 per cent, LOG NORMAL MODEL

P 1026

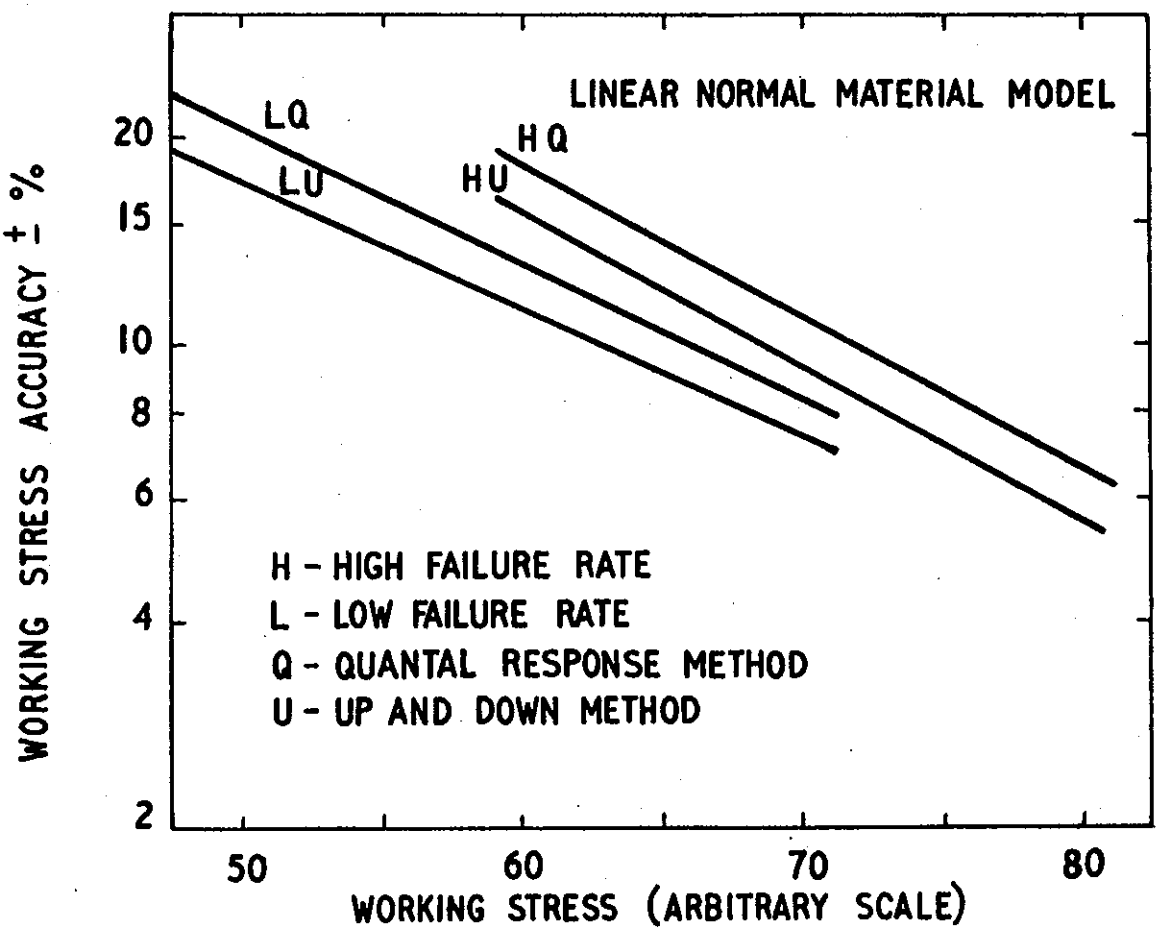

FIGURE 9. VARIATION OF ACCURACY OBTAINED FROM A SAMPLE SIZE OF 200, LINEAR NORMAL MODEL

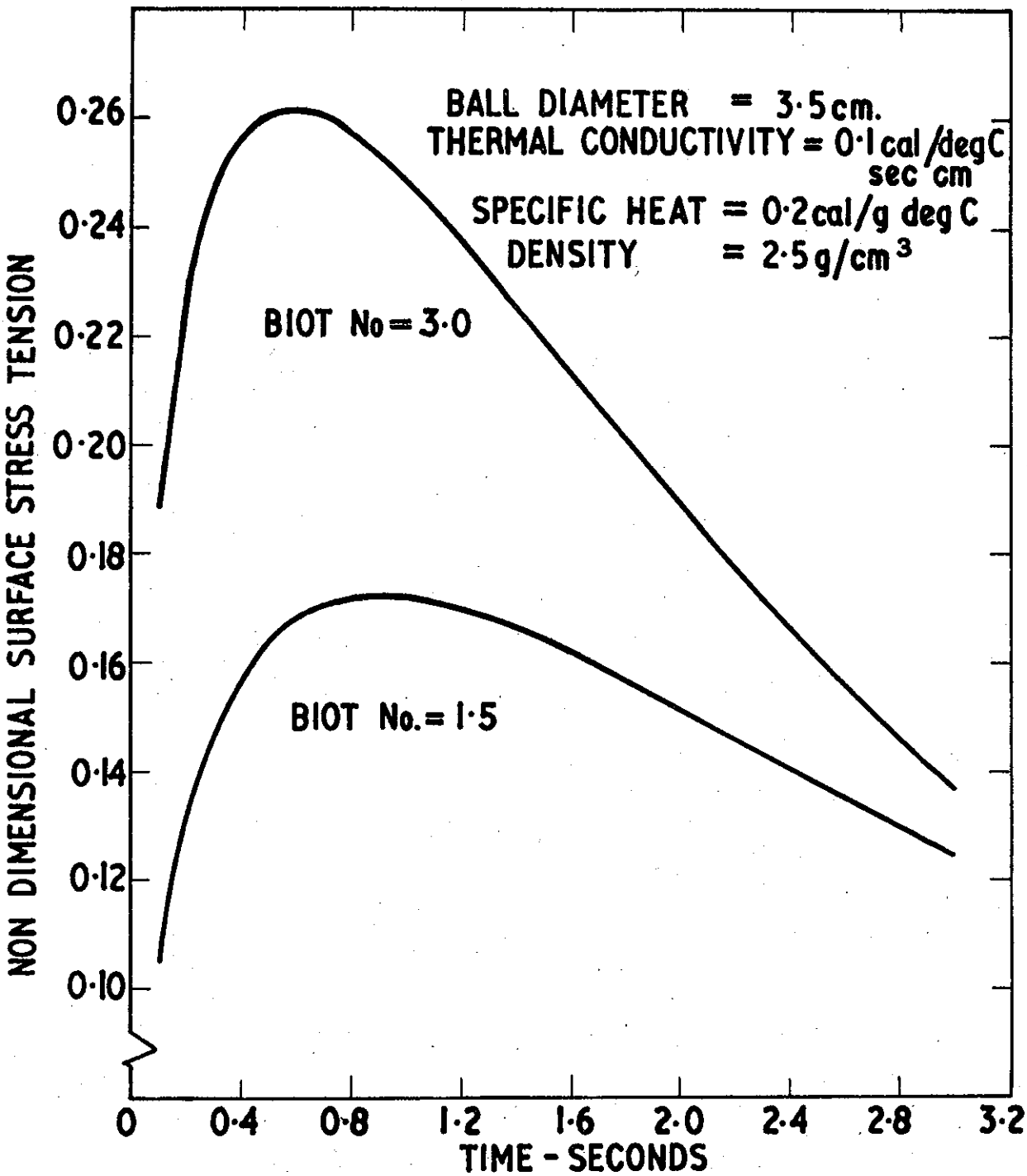

FIGURE 10. SINGLE SPECIMEN SURFACE STRESS HISTORY

P 1026

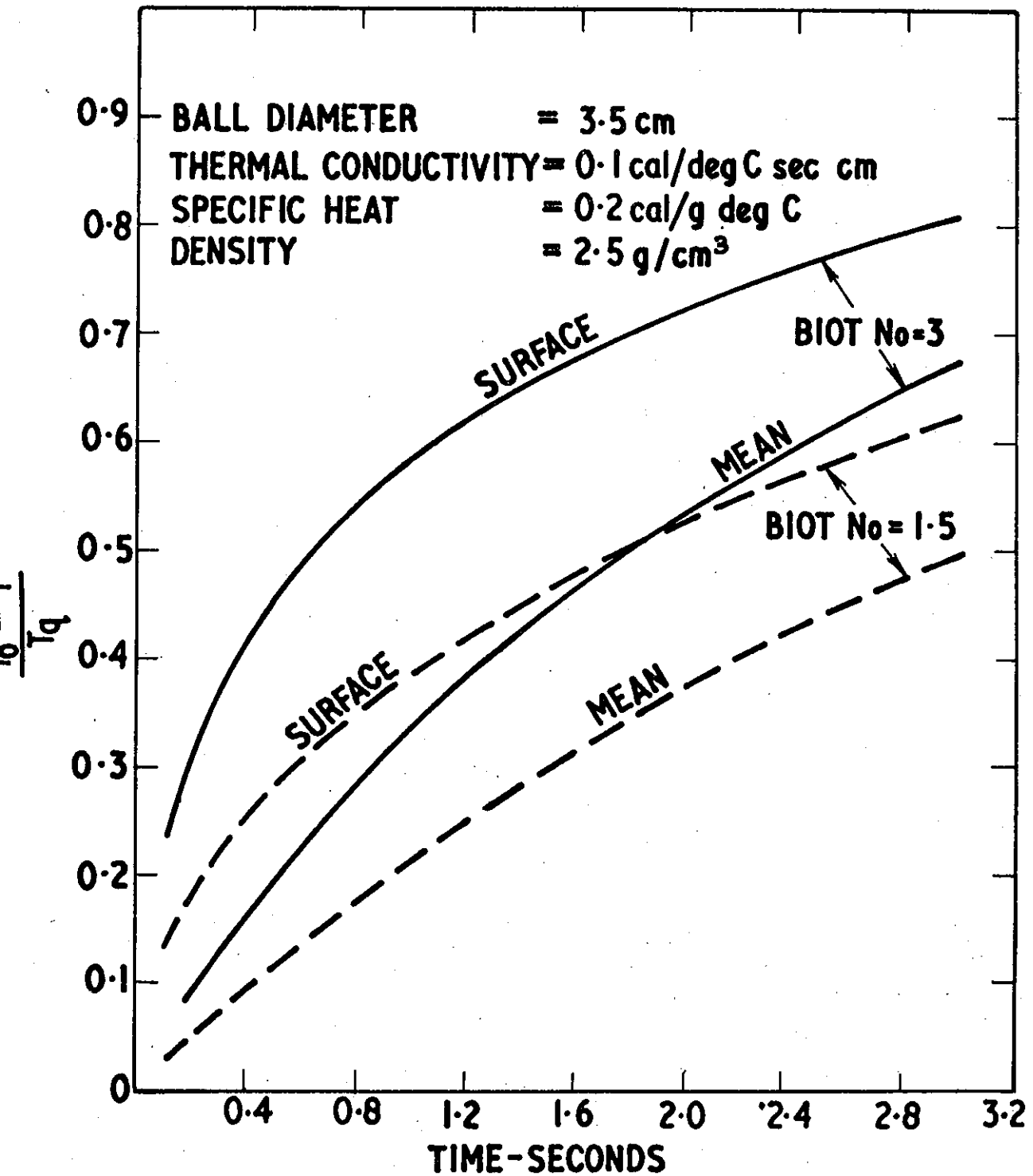

FIGURE 11. SINGLE SPECIMEN TEMPERATURE HISTORY

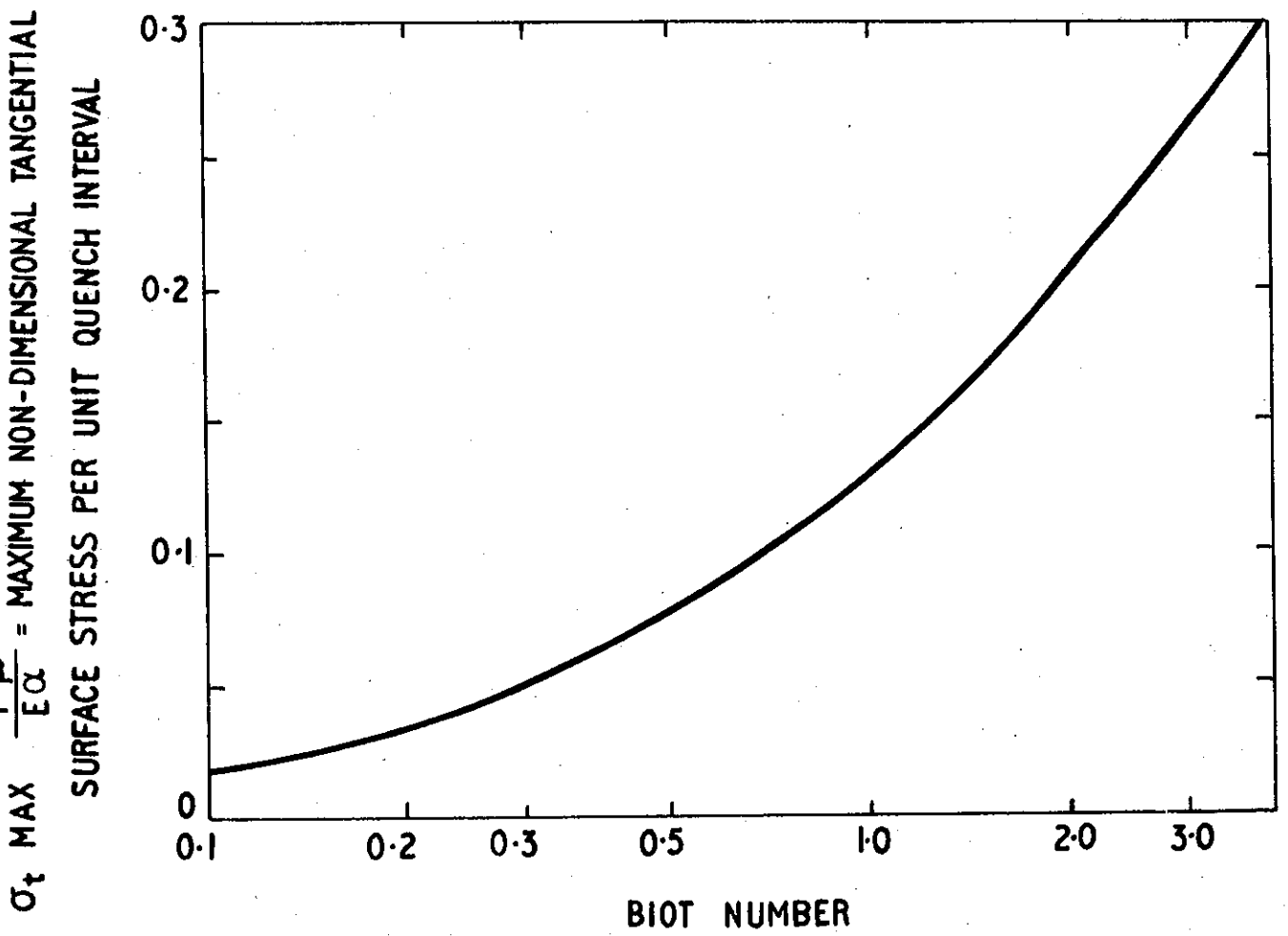

FIGURE 12. VARIATION OF MAXIMUM SURFACE STRESS WITH BIOT NO.

P 1026

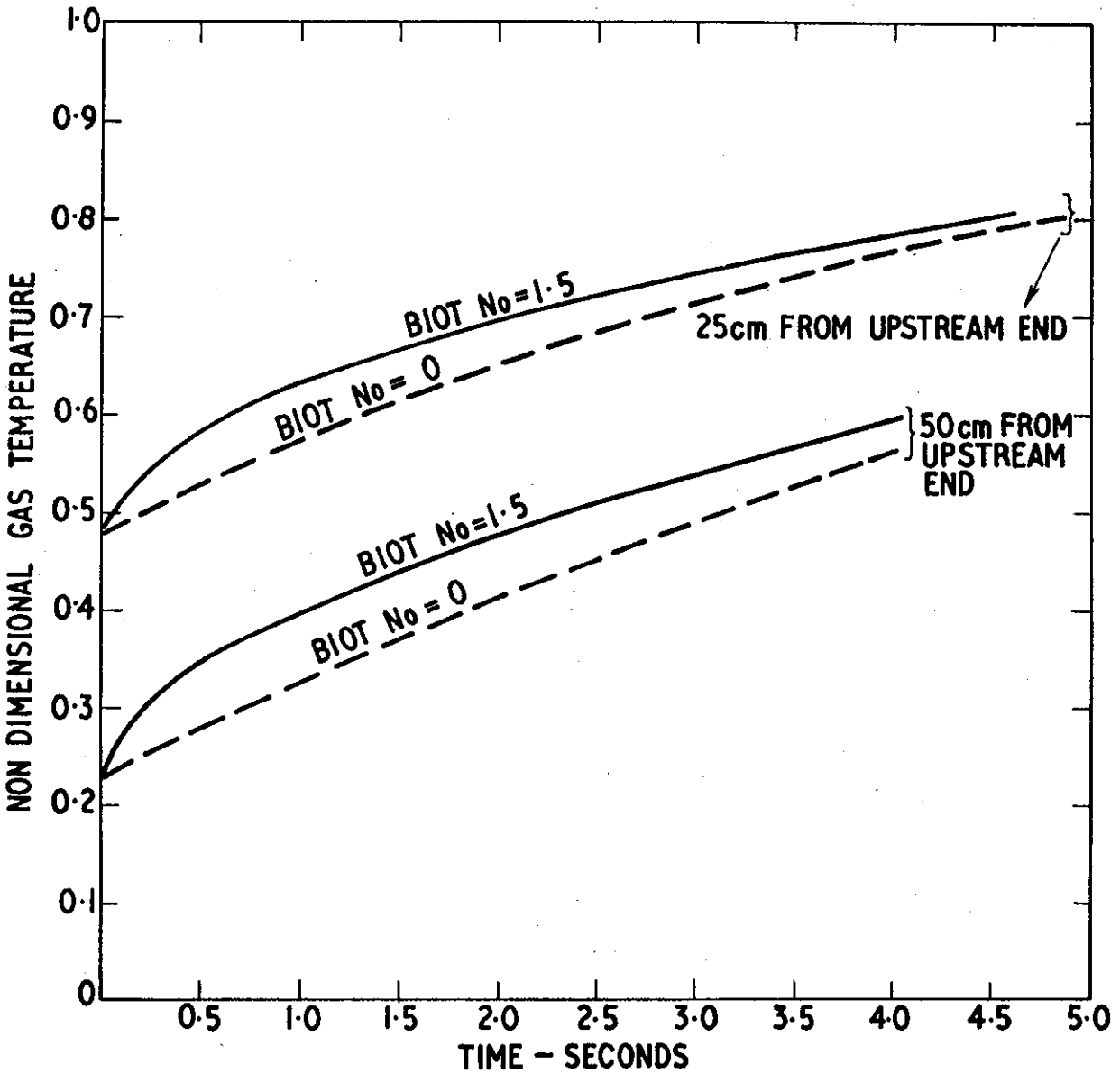

FIGURE 13. GAS TEMPERATURE HISTORIES FOR THE STANDARD CASE (BIOT NO. = 1.5) AND THE INFINITE THERMAL CONDUCTIVITY CASE (SCHUMANN'S ANALYSIS, BIOT NO. = 0)

P 1026

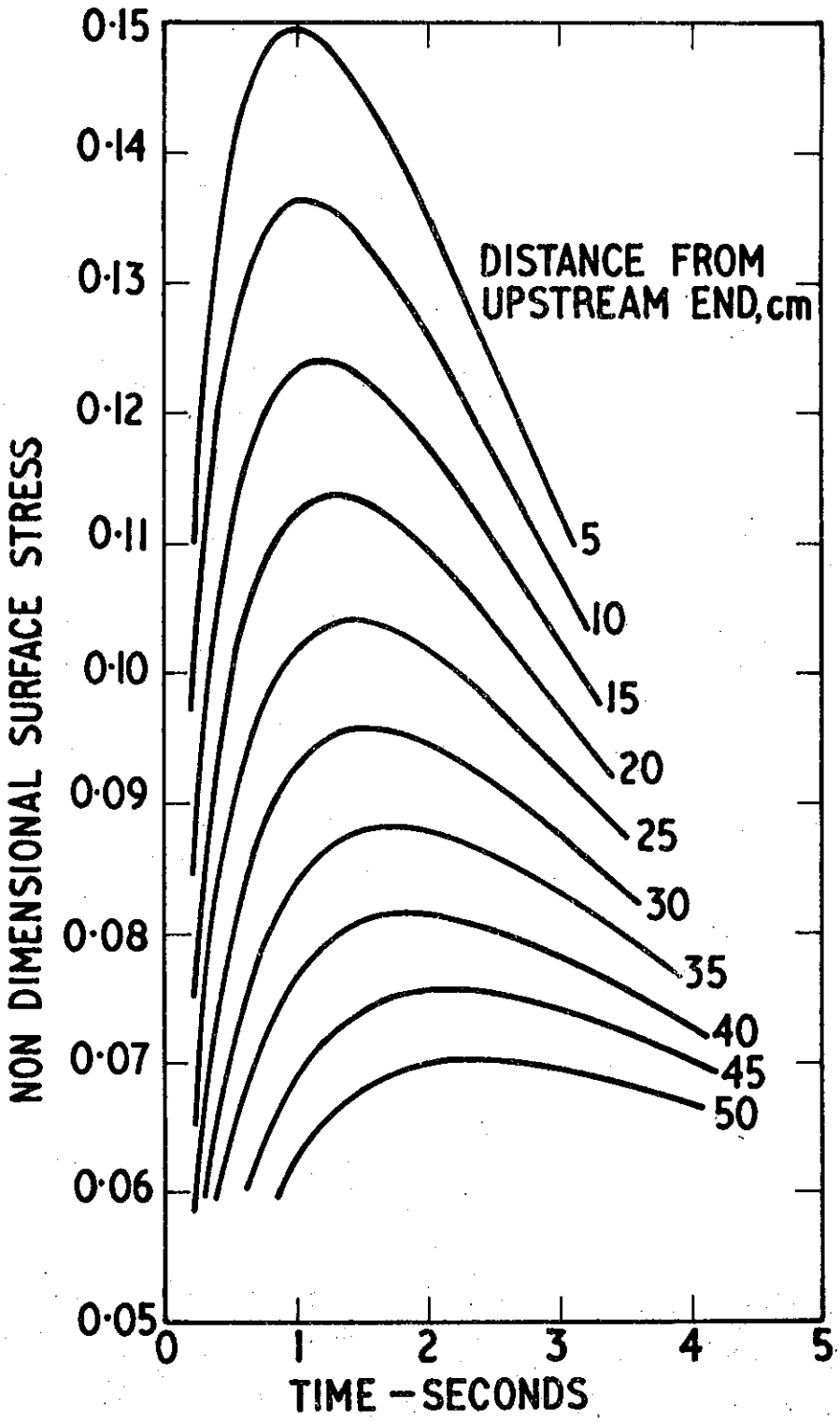

FIGURE 14. SURFACE STRESS HISTORY FOR THE STANDARD CASE, BIOT NO. 1.5

P 1026

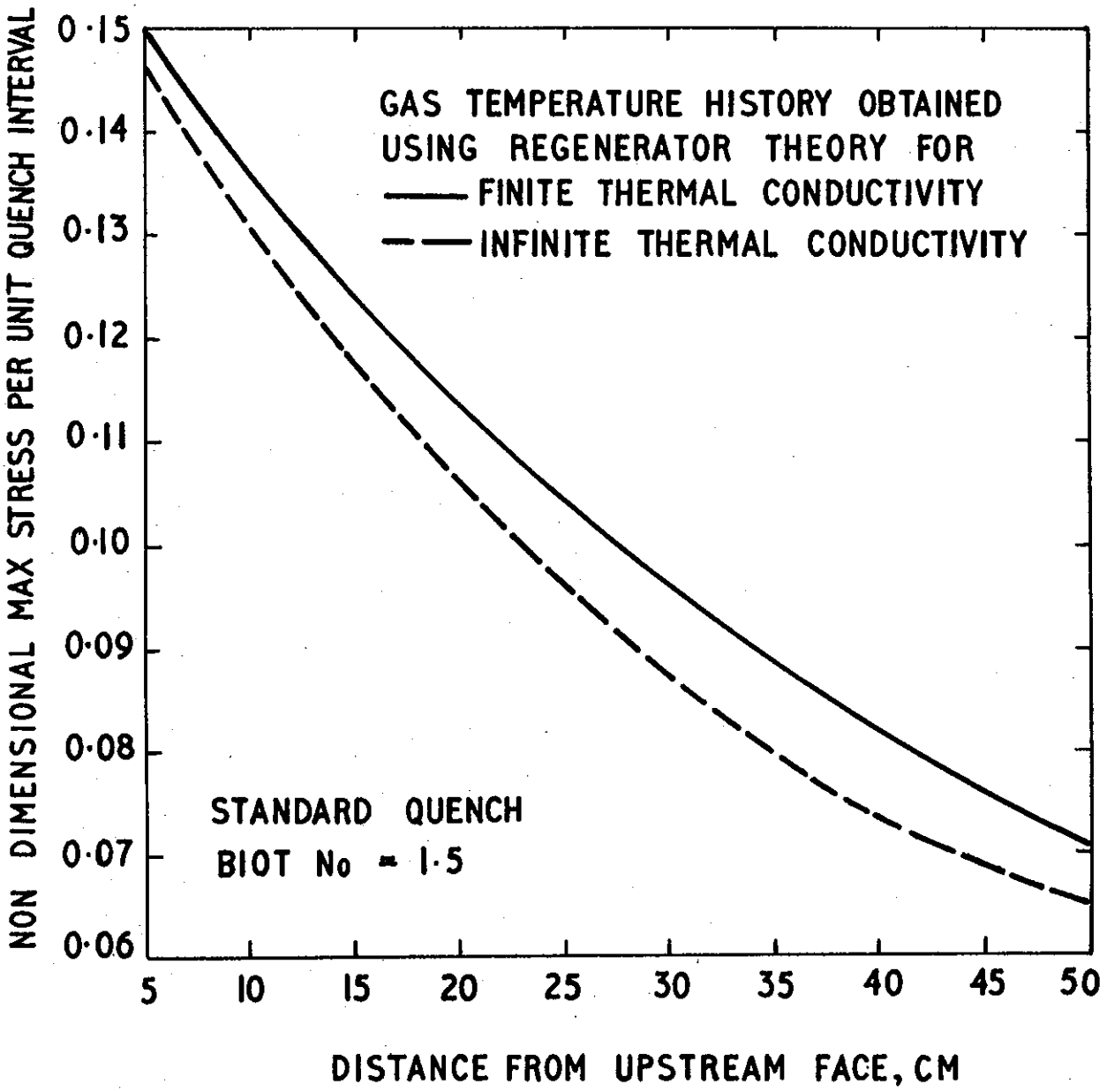

FIGURE 15. VARIATION OF MAXIMUM STRESS ALONG A QUENCHED MULTIPLE SPECIMEN, BIOT NO. = 1.5

P1026

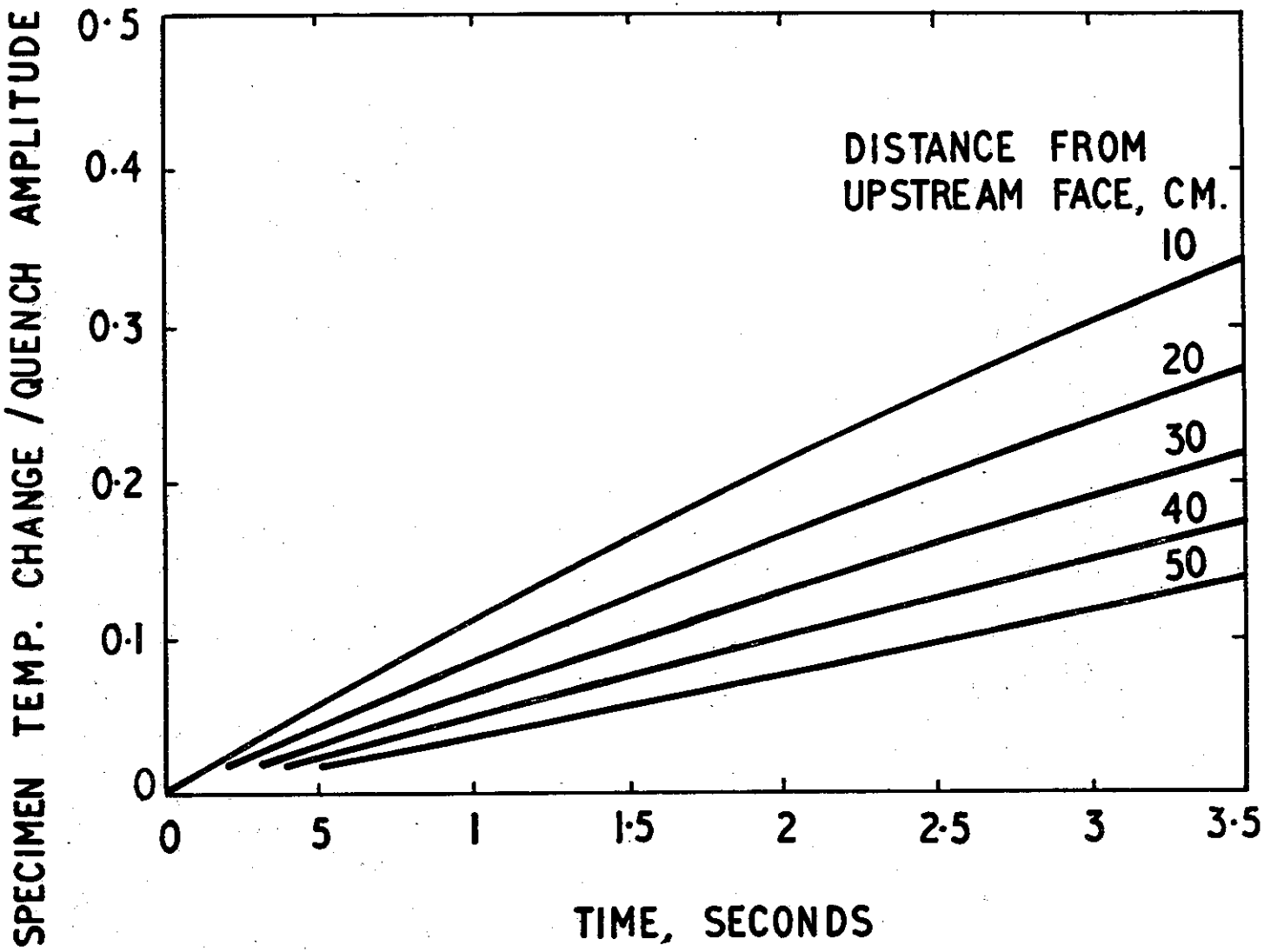

FIGURE 16. MEAN TEMPERATURE HISTORY OF COPPER CALIBRATION SPECIMEN UNDER STANDARD CASE CONDITIONS, BIOT NO. = 0.15

P 1026

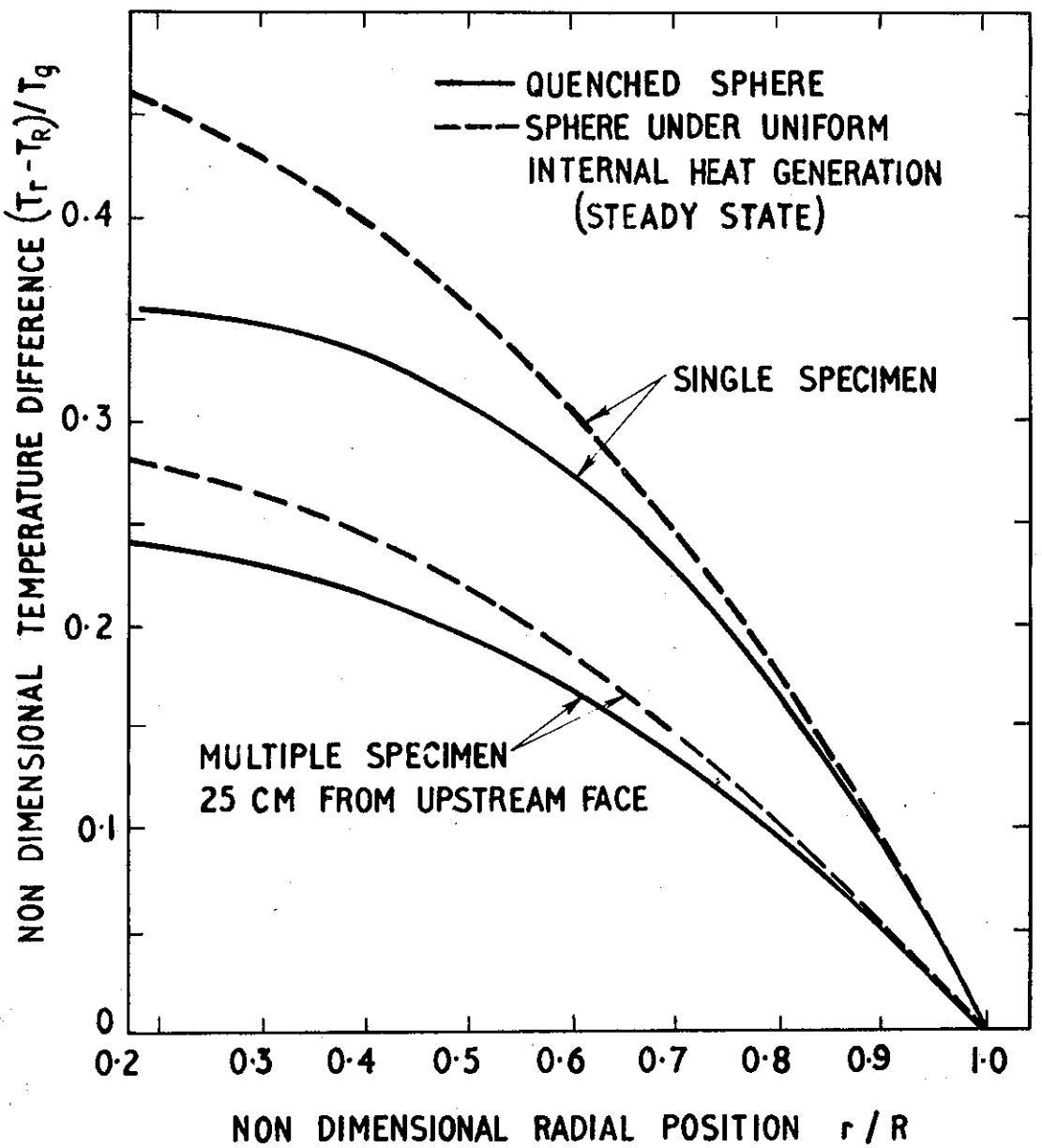

FIGURE 17. COMPARISON OF THE TEMPERATURE DISTRIBUTIONS AT THE INSTANT OF MAXIMUM STRESS IN QUENCHED SPHERES TO THE DISTRIBUTION IN A SPHERE UNIFORMLY GENERATING HEAT INTERNALLY IN THE STEADY STATE

P1026